



# Connecting volcanic climate impacts to famine in China using the REACHES database

Richard Warren<sup>1,2</sup>

<sup>1</sup>Institute of History, University of Bern, Bern, CH-3012, Switzerland

5 <sup>2</sup>Oeschger Centre for Climate Change Research, University of Bern, Bern, CH-3012, Switzerland

*Correspondence to:* Richard Warren ([richard.warren@unibe.ch](mailto:richard.warren@unibe.ch))

**Abstract.** Volcanic eruptions have been linked to historical famines in many parts of the world. In China, reduced temperatures following major eruptions can destabilise the hydroclimate and agricultural production, contributing to subsistence crises and even the downfall of dynasties. This study provides the first long term analysis of the specific connection between volcanic activity and famine in eastern China from 1440 to 1900 CE. Using the REACHES historical climate database, it reconstructs indices measuring temperature, drought, flooding, crop failure and famine. Superposed epoch analysis of these indices reveals a recurring, though regionally distinct, association between eruptions and famine. Famine peaks occur in northern China in the year of an eruption, in central China one to three years later - coinciding with delayed drought and crop failure - and in southern China in the first post-eruption year. Correlation analysis indicates statistically significant relationships between volcanic forcing, hydroclimatic extremes, crop failure and famine. Case studies – including a new assessment of the impacts of the 1809 “unknown” eruption – demonstrate how other factors, such as the El Niño Southern Oscillation, non-volcanic climate processes, price volatility, disease and state relief mediate volcanic impacts. Many of these factors form feedback loop than can delay, amplify or counteract volcanic effects. We conclude that while eruptions may not be the primary drivers of famine in China, they significantly increase the risk of drought, flood, harvest failure and subsequent subsistence crises. The findings demonstrate the capacity of major volcanic events to destabilise food systems through coupled climatic and societal pathways.

## 1 Introduction

In many parts of the world, famines have been linked to major volcanic eruptions (Brönnimann and Krämer, 2016; Toohey et al., 2016; Huhtamaa et al., 2022; Kim, 2025). Volcanic sulphate aerosols cool global temperatures and disrupt regional rainfall patterns, which can negatively affect both agriculture and food prices. Whether this is the case in China is still an open question Evidence from early Chinese history suggests that volcanic eruptions are associated with cold, drought and locust outbreaks, but only inconsistently to harvests and subsistence crises (Yang and Ludlow, 2025). Research on later periods has identified links between volcanoes and dynastic collapse (Gao et al., 2021a), climate and famine (Lin et al., 2020; Wei and Li, 2024) and eruptions and the Chinese climate (Gao and Gao, 2018; Chen et al., 2020; Liu et al., 2022; Zhuo et al., 2023). However, a persistent connection between volcanic activity and famine has not been systematically investigated. This study addresses this



30 gap by assessing the climatic, environmental and societal pathway volcanic eruption to famine across 460 years of Chinese history, 1440 to 1900 CE.

The impact of volcanic eruptions on the East Asian climate has been addressed by several studies, using a variety of climate proxies and climate modelling data. Tropical volcanic eruptions tend to coincide with drying in south China in the year of an eruption, wetting in north and central China one year after the eruption, and regional wetting effects three years after the eruption (Gao and Gao, 2018). This is modulated by volcanic interactions with the El Niño Southern Oscillation (ENSO), which can reverse the regional drying, resulting in a general wetting effect when an a El Niño is induced by or coincides with a volcanic eruption (Liu et al., 2022). The physical mechanism behind the volcanic impacts is argued to be a weakening of the East Asian summer monsoon (EASM), due to a reduced land sea thermal gradient (Chen et al., 2020), and a strengthening of the East Asian subtropical westerly jet stream as it moves south (Gao and Gao, 2018). Heterogeneous moisture transport, cloud formation and feedbacks between clouds and soil moisture can all modify these effects leading to diverse hydrological effects in different regions of China (Chen et al., 2020; Zhuo et al., 2023). The location of the eruption can also change its impact, with northern hemisphere eruptions having a considerably bigger drying impact than southern hemisphere eruptions (Zhuo et al., 2023). The impact of ENSO, separate to an eruption, appears to be less than that of volcanic events and quite regionally specific. Modern studies show drought is most strongly correlated with ENSO in the south east of China (Lv et al., 2022), but the biggest agricultural impacts are in the north and central eastern China - around Shanghai and Henan province - where both El Niño and La Niña can have a positive effect on crop yields (Li et al., 2020).

Recent research has also examined the links between climate variability and famine in China. Using the REACHES database, Lin et al. (2020) found that during the Qing Dynasty (1644-1911), famine and drought tends to be concentrated in three different epicentres: the lower Yellow River (in northern China); the lower Yangtze River (in central China); and occasionally in the far south of China along the Pearl River. From these centres, famines sometimes spread further inland to the upper reaches of the Yellow and Yangtze rivers. Famines were usually strongly connected to drought, but also to crop failure, price fluctuations and social turmoil, as well as disaster relief and locusts. Colder periods also tended to see lower agricultural yields and more social instability. Further analysis of these relationships was conducted by Wei and Li (2024) using Chinese historical data sources and climate reconstructions. They found both coincidence and correlation between annual drought, flood and famine in Qing Dynasty China. The strongest correlations were observed between drought and famine in northern China, while in southern China famine was correlated with both drought and flood, albeit more weakly than in the north. Notably, lagged analyses revealed strong correlations between drought and famine at one- and five-year intervals across China as a whole, suggesting the influence of ENSO or other delayed feedback mechanisms.

The broadest picture studies link volcanic eruptions directly to famine and other sociopolitical events. Gao et al. (2021a) connected volcanic impacts to Chinese dynastic collapse, finding that over the last 2000 years, warfare and regime change



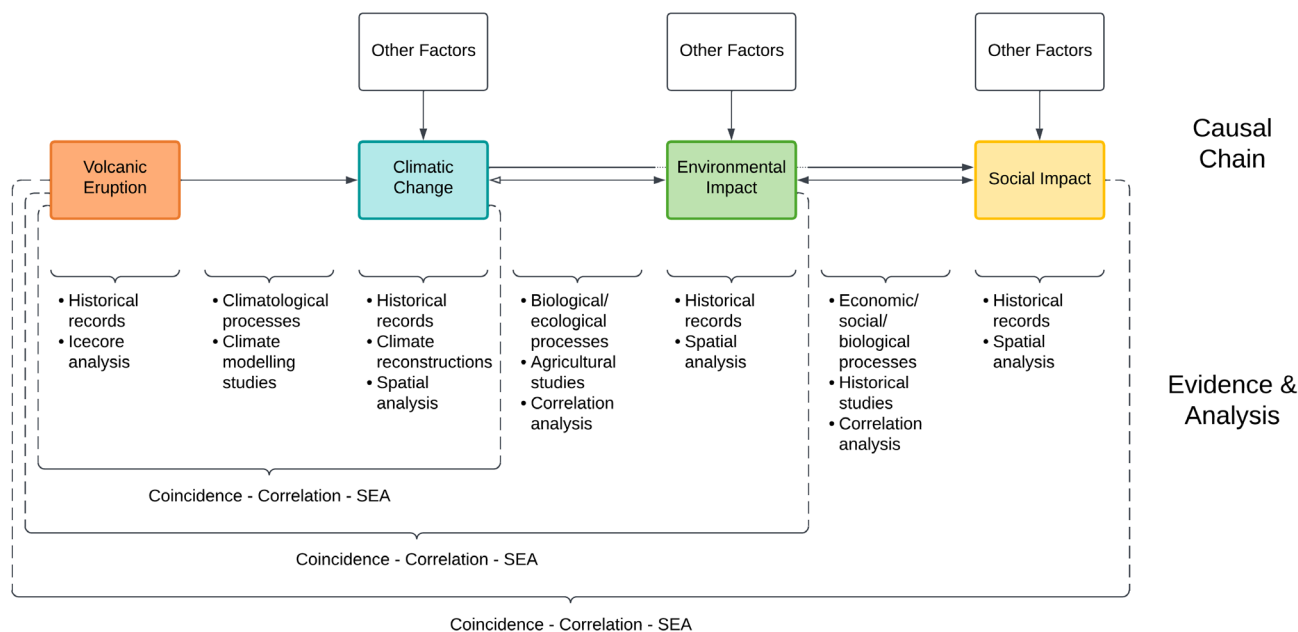
coincided with major eruptions considerably more often than would be expected from random chance. They hypothesized that agricultural disruption and resulting subsistence stress, together with the symbolic impact of ominous portents, adverse weather, and volcanically induced lunar and solar phenomena may have weakened the mandate and legitimacy of Chinese rulers. This brought to light the importance of not only material impacts, but also perception and meaning as important factors shaping the societal consequences of volcanic eruptions in the Chinese context. This was also emphasized by Yang and Ludlow (2025), although they pointed out that, at least in early Chinese history, this could have both positive and negative effect on disaster relief. More specific case studies, investigating the impact of single eruptions, have connected the Laki eruption in Iceland (1783) to drought, locust outbreaks and famine in eastern China (Gao et al., 2021b); the Tambora eruption in Indonesia (1815) to unusually cold conditions in southern China, although with minimal social impacts (Gao et al., 2017); the Parker eruption in the Philippines (1640) to a prolonged and severe drought that potentially contributed to the collapse of the Ming dynasty (Chen et al., 2020); and a major unidentified eruption in 535 or 536 to summer frosts, multi-year drought, crop failures and catastrophic famines (Pankenier, 2022).

The connection between eruptions and agriculture, and agriculture and famine, is perhaps the least well evidenced, since it is often assumed. Agriculture in China is complex, with regional variation in dominant crops and cropping intensity (Tian et al., 2015; Yin et al., 2024). Nevertheless, Hao et al. (2020) found that since the beginning of the 19th century decreased harvest yields in southwest China have been consistent with periods of declining temperatures, higher drought occurrence and low-latitude volcanic eruptions. They also emphasised the importance of social resilience and relief measures in shaping the ultimate impacts of subsistence crises. This is consistent with the results from Lin et al. (2020) and with the broader scholarship on famine and agriculture, the most well know being Sen (1982) who argued that prices and human responses (entitlements) are often more important than actual production in determining the outcome of famines.

## 2 Data and Methodology

### 2.1 The VICES approach

This paper broadly follows the systems approach introduced in (Warren, 2026). This has since been developed, based on other volcano-society interaction frameworks (Brönnimann and Krämer, 2016; Ljungqvist et al., 2021; Büntgen et al., 2025) into the more detailed Volcanic Impacts on Climate, Environment and Society (VICES) approach - see Fig. 1.



90

**Figure 1. Conceptual diagram showing the VICES approach to studying volcano-climate-society interactions, including the proposed causal chain linking volcanic eruptions to social impacts and the evidence and analysis used to assess/reconstruct each impact and connection.**

95 The approach starts by noting the basic coincidence of famine in China and global volcanic activity, particularly in the 1580s, 1640s, and 1830s (Fig. 3). We then assess whether such coincidences are repeated and statistically significant using correlation and superposed epoch analysis (SEA). The effects of the El Niño Southern Oscillation (ENSO) - the primary ‘other factor’ affecting the Chinese climate on an interannual timescale (Li et al., 2020; Lv et al., 2022) - are similarly investigated. Next, we evaluate whether the proposed causal pathway - from volcanic eruption to climate disruption to agro-environmental impacts to famine - is supported by correlations between the relevant variables. Following Yang and Ludlow (2025), we then combine our long-term statistical analysis with detailed historical case studies to reconstruct the factors that moderate this pathway. Case studies include a new assessment of the impact on China of the 1809 ‘unknown’ eruption, as well as previous research on the Parker (1641), Laki (1783) and Tambora (1815) eruptions.

## 2.2 Selecting major historical eruptions and ENSO years

105 To identify volcanic eruptions with a global climate impact, we utilise the Toohey and Sigl (2017) stratospheric aerosol optical depth (SAOD) dataset, based on ice core composites from Antarctica and Greenland. Major volcanic eruptions were categorised as those with a peak global mean SAOD of over 0.75, giving a sample of 13 eruptions between 1440 and 1900 CE (see Table 1). The 20<sup>th</sup> century eruption of Mt. Pinatubo (1991) has been included for reference.



110 **Table 1. Summary information on the 13 major volcanic eruptions used in this study. The data is sourced from Toohey and Sigl, 2017.**

<i>Volcano</i>	<i>Eruption Year</i>	<i>Peak Forcing Year</i>	<i>Peak Global Mean SAOD</i>	<i>Volcano Latitude</i>
Unidentified	1453*	1453	0.106	N Hemisphere*
Kuwaë**	1457	1458	0.307	-16.83**
Colima	1585	1585	0.090	19.51
Nevada del Ruiz	1595	1596	0.077	4.89
Huaynaputina	1600	1600	0.178	-16.61
Parker	1640	1641	0.208	6.11
Unidentified	1695	1695	0.173	Tropical
Laki	1783	1784	0.187	64.4
Unidentified	1809	1809	0.200	Tropical
Tambora	1815	1816	0.255	-8.25
Zavaritskii***	1831	1831	0.135	46.91***
Cosiguina	1835	1835	0.105	12.98
Krakatau	1883	1884	0.112	-6.10
<i>Pinatubo</i>	<i>1991</i>	<i>1992</i>	<i>0.106</i>	<i>15.14</i>

Further information was acquired from \*Burke et al., 2023, \*\*Ro et al., 2025, \*\*\*Hutchison et al., 2025.

115 To investigate the effects of ENSO, extreme El Niño and La Niña years were identified using the Zhu et al. (2022) Niño 3.4 reconstruction. This dataset combines tree ring chronologies with coral proxies to reconstruct sea surface temperature (SST) anomalies over the central Pacific Niño 3.4 region. Years with SST anomalies exceeding the 95th percentile were classified as extreme El Niño events, while years below the 5th percentile were classified as extreme La Niña events. This resulted in a set of 20 El Niño years and 19 La Niña years - see Table 2.

120

**Table 2. Extreme El Niño and La Niña years between 1440 and 1900 CE, identified from the Zhu et al. (2022) ENSO reconstruction.**



<i>El Niño Years</i>	<i>Niño 3.4 [K]</i>	<i>La Niña Years</i>	<i>Niño 3.4 [K]</i>
<b>1485</b>	1.313	<b>1455</b>	-1.375
<b>1499</b>	0.875	<b>1464</b>	-1.375
<b>1526</b>	0.875	<b>1495</b>	-1.188
<b>1606</b>	0.813	<b>1506</b>	-1.375
<b>1609</b>	1.063	<b>1626</b>	-1.813
<b>1629</b>	1.063	<b>1650</b>	-1.438
<b>1719</b>	0.875	<b>1663</b>	-1.375
<b>1747</b>	1.313	<b>1685</b>	-1.500
<b>1759</b>	1.250	<b>1716</b>	-1.188
<b>1764</b>	0.813	<b>1725</b>	-1.313
<b>1792</b>	1.250	<b>1742</b>	-1.563
<b>1800</b>	1.000	<b>1806</b>	-1.313
<b>1804</b>	1.188	<b>1847</b>	-1.313
<b>1828</b>	0.813	<b>1861</b>	-1.563
<b>1833</b>	0.813	<b>1871</b>	-1.188
<b>1839</b>	1.250	<b>1879</b>	-1.750
<b>1869</b>	1.625	<b>1887</b>	-1.500
<b>1878</b>	1.563	<b>1890</b>	-1.375
<b>1885</b>	0.875	<b>1893</b>	-1.625
<b>1889</b>	0.813	<b>1899*</b>	-1.438

\*These years were excluded from the SEA, as the event year + 5 was outside of our data range.

To account for the inherent uncertainty in ENSO reconstructions, the analysis was repeated using two alternative  
 125 reconstructions (Li et al., 2013; Dätwyler et al., 2019) based on different methods and data sources (see Appendix A).

### 2.3 Historical indices and the REACHES database

To reconstruct the potential climatological, environmental and social impacts on China, this study uses the REACHES  
 database, a digitised database of Chinese meteorological and climate related records from 1368 to 1911 CE (Wang et al., 2018).  
 REACHES compiles and categorises an extensive set of official and local records from across China, originally collected in *A*  
 130 *Compendium of Chinese Meteorological Records of the Last 3,000 Years* (Zhang, 2013). From these, a study area of twenty-  
 three provinces was selected, chosen for having a sufficiently large number of observations in the REACHES database (Fig.  
 2c). These provinces were divided into three regions (Fig. 2a), based on climatology (Wang et al., 2024), agriculture (Li et al.,  
 2024), and historically concurrent famines (Lin et al., 2020). The study period 1440 to 1900 was chosen to include as many  
 large volcanic eruptions as possible (particularly the 1452 eruption) whilst ensuring that all regions had enough reports for  
 135 statistical analysis (Fig. 2b).

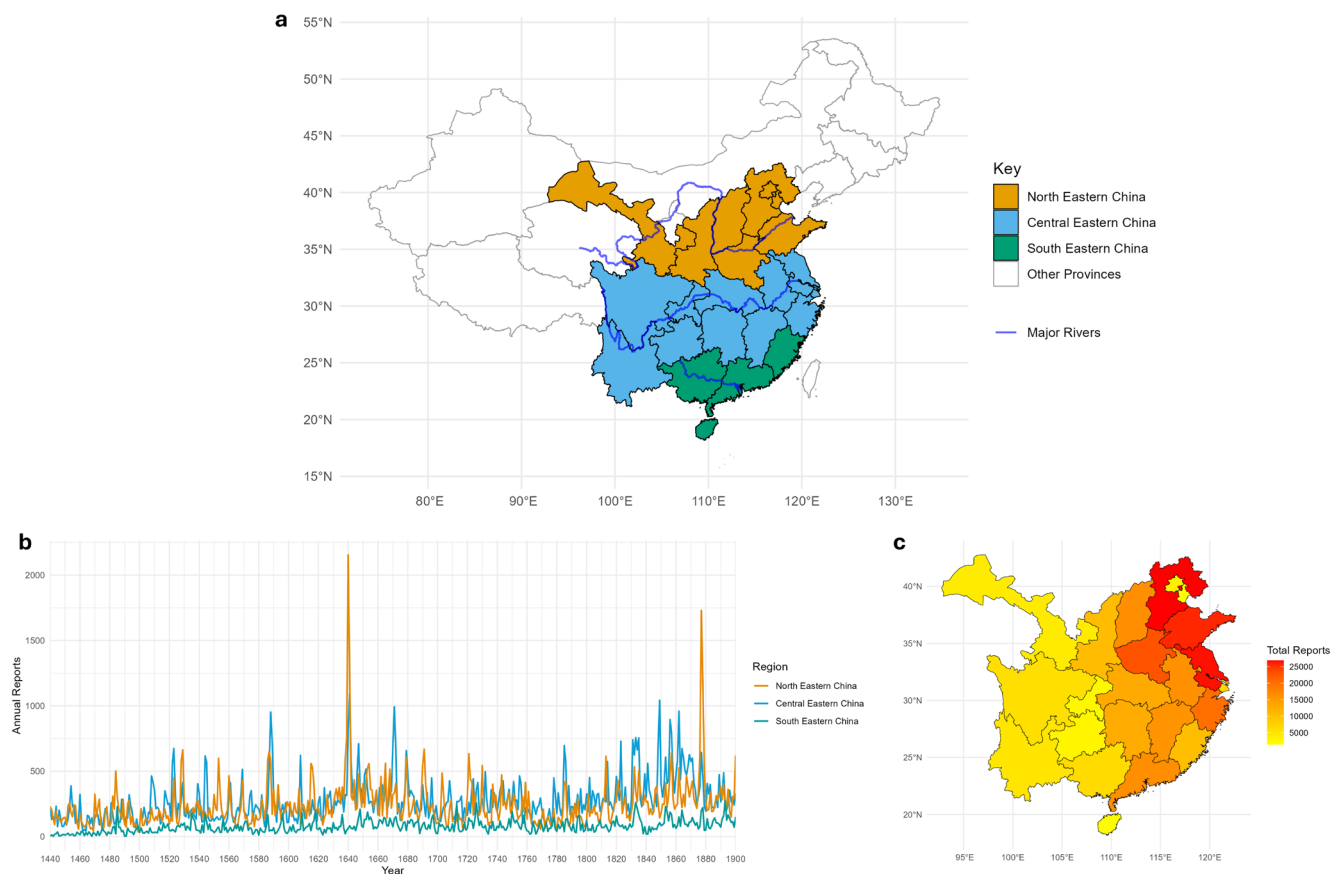


**Figure 2. (a) Map of China showing the provinces included in this study and approximate routes of major river systems. Provinces are divided into regional divisions as follows: North Eastern China = Hebei, Beijing, Tianjin, Shandong, Henan, Shanxi, Shaanxi, and Gansu; Central Eastern China = Jiangsu, Anhui, Hubei, Shanghai, Zhejiang, Jianxi, Hunan, Sichuan, Chongqing Guizhou and Yunnan; South Eastern China = Fujan, Guangdong, Hainan, and Guangxi. The major rivers are the Yellow River in northern China, Yangtze River in central China and Pearl River in the south. (b) Total number of reports per year in the REACHES database for each region, 1440 to 1900 CE. (c) Total reports per province, 1440 to 1900 CE.**

145 Within REACHES, each record is categorised according to subject (famine, drought, flood, crop failure, price fluctuation, locusts, social turmoil, disease, famine relief etc.), along with a type description. To account for the variation in the number of reports over time and between regions, these records were converted into an event index using Eq. (1).

$$Event\ Index = \frac{Total\ Number\ of\ Event\ Reports}{Total\ Number\ of\ Reports*} \quad (1)$$

\*100 year moving average

150 Note that all values are *per region*. This formula was applied to reports of famine, drought, flood, crop failure to produce a famine index (FAI), drought index (DI), flood index (FI) and crop failure index (CFI) for each region. The event index assumes



that a higher number of reports indicates a more widespread and long-lasting event. This interpretation is supported by the general homogeneity of magnitude and duration classifications within the REACHES reports.

155 Based on modern Chinese agricultural studies (Li et al., 2024; Feng et al., 2025), the two main climate factors affecting crop growth in China are summer temperatures and spring/summer precipitation. However, Lin et al. (2020) found a stronger connection between droughts and crop failure than between precipitation and crop failure. We therefore measure the climate impact from volcanic eruptions using the drought index (DI) based on the REACHES data and the summer temperature reconstruction from Wang et al. (2024) (also based on REACHES). This temperature reconstruction covers the extended  
160 summer period, May to September, which includes much of the growing season in China (Li et al., 2024; Feng et al., 2025). Since Wang et al. used smaller regions than our own, their results were averaged across each study region to create a new regional summer temperature index (STI).

#### 2.4 Statistical and spatial analysis

Superposed epoch analysis (Robock and Mao, 1995) is a statistical method used to study the temporal response of a variable  
165 or system to repeated events, such as the impact of volcanic eruptions on climate, agriculture or society (Gao et al., 2021a; Huhtamaa et al., 2022; Zhuo et al., 2023). We use this method to present the composite effects of 13 major eruptions (see Figs. 4 & 5) over an 11 year window, ranging from 5 years prior to each eruption to 5 years following. To test significance, a Monte Carlo model test (Zhuo et al., 2023) was employed, whereby 10,000 resamples of the original data are made and the mean and 95% confidence band of this sample are identified. A p-value test (Bunn et al., 2025) with a different resampling was also used  
170 to show the probability that each result occurred by random chance. Values that were both outside of the 95% confidence band and had a p-value of  $<0.05$  were considered statistically significant.

Correlation analysis employing both Pearson and Spearman's Rank correlation coefficients was used to capture linear and non-linear relationships between variables (Table 4 & Appendix G).

175 For the 1809 case study, we use spatial plots to show distribution and prevalence of drought, flood and famine, and related biological, economic and social phenomena for the years 1808 to 1812 (see Fig. 6). Following the method used by Gao et al., 2017 and Lin et al., 2020, we first collected all the relevant records from REACHES and then converted them into geo-referenced points showing the location and severity of crop failure, locusts, price fluctuations, social turmoil, disease and  
180 disaster relief. The distribution of drought and famine records was shown using a kernel density plot – a method used to create a probability density function and contour plot from point variables (see Lin et al., 2020; Ripley et al., 2025).



### 3 Results

#### 3.1 Index comparison

Figure 3 gives an overview of the REACHES index data for summer temperature, drought, crop failure and famine, highlighting the potential role of volcanic eruptions.

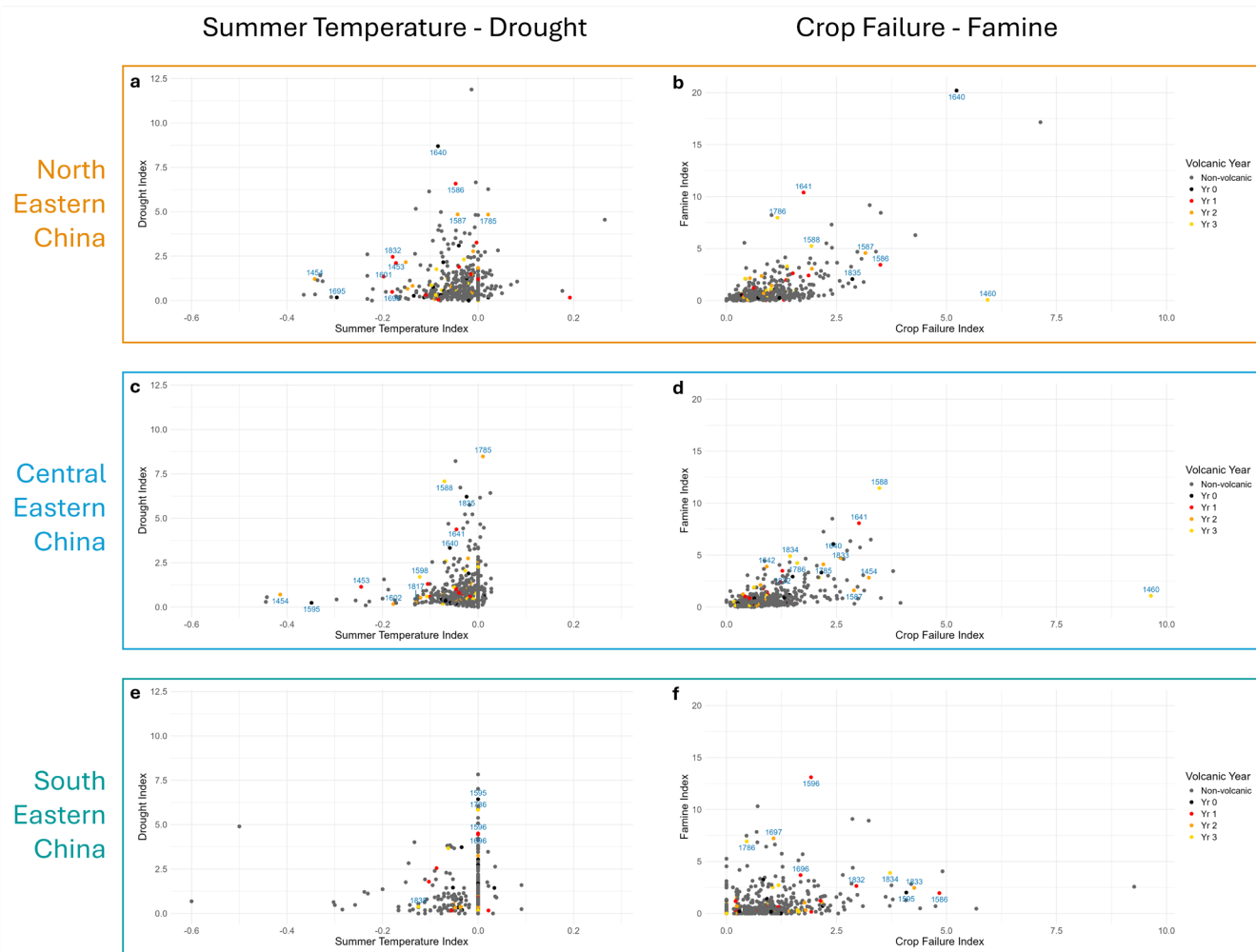


**Figure 3.** Scatterplots showing the distribution of STI, DI, CFI and FAI in north, central and south eastern China for volcanic and non-volcanic years. Labeled points are the years following major eruptions that are also in the top 5% of years in either index. See Appendix B for the equivalent graphs showing STI-FAI, DI-FAI and FI-FAI.

190

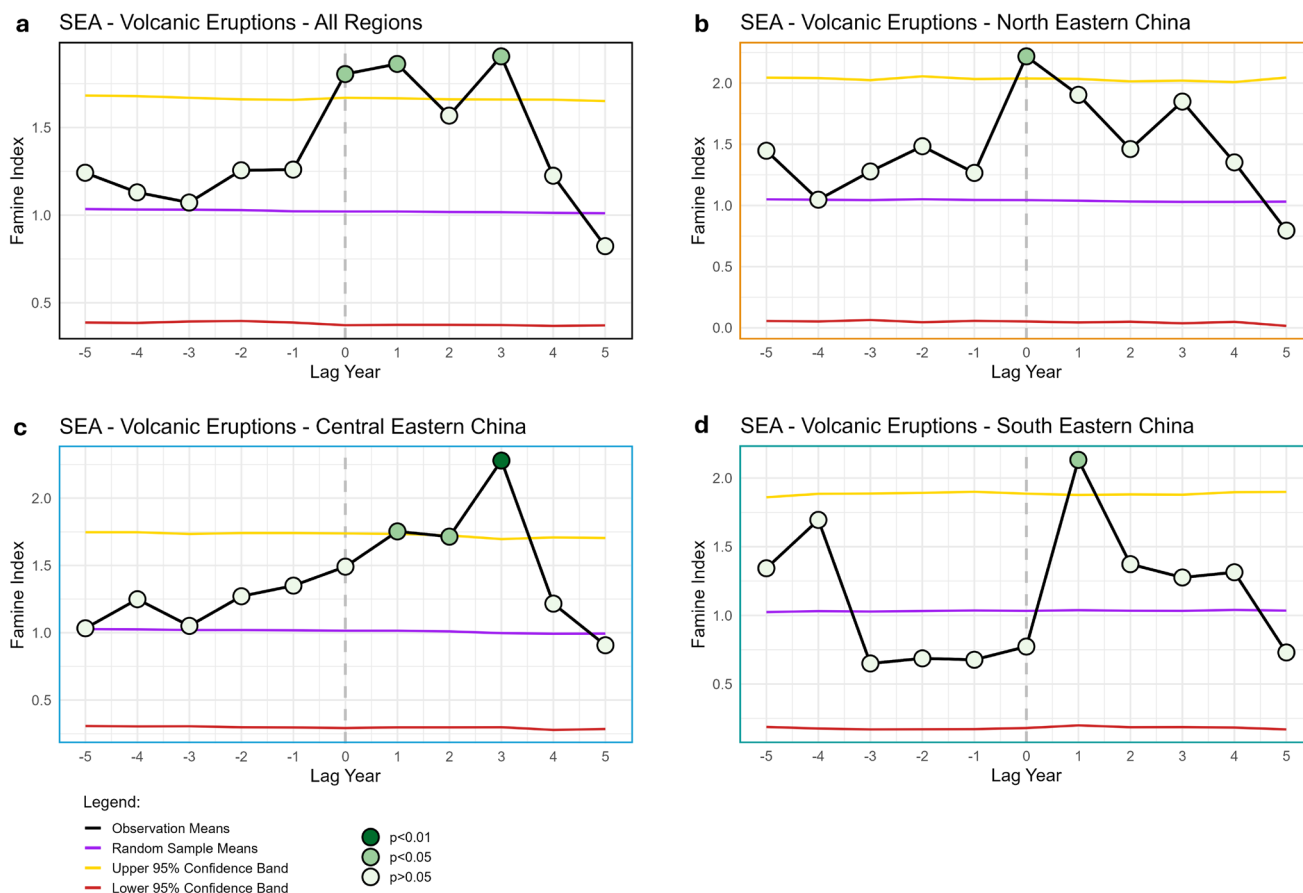
The plots show that while some eruptions coincide with extreme temperatures, droughts, crop failures, and famines, the majority of extreme years are not associated with volcanic activity. This picture is fairly consistent across all three regions of China. Hence, barring any effects more than three years post-eruption, it seems that volcanism can at best only partly explain



the occurrence of famine in China. However, this general finding may mask some underlying trends, and enough extreme years do coincide with volcanic years to merit further investigation.

### 3.2 Superposed epoch analysis

To test whether the coincidence of famine events with major volcanic eruptions is statistically significant, we turn to SEA analysis (Fig. 4).



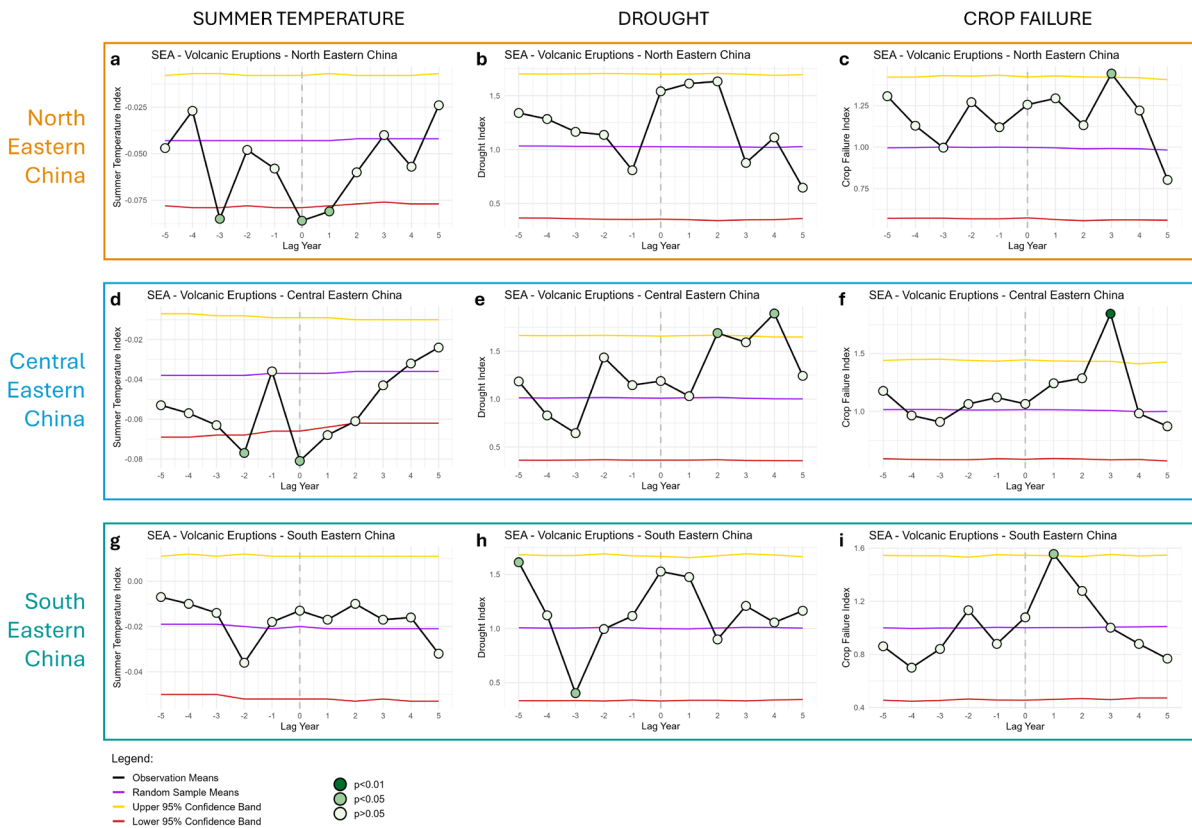
200 **Figure 4. Superposed epoch analysis showing famine index (FAI), relative to eruption years, for the three study regions. Purple, yellow and red lines show the mean and 95% confidence band for the Monte Carlo resampling (10,000 iterations). Note that the p values are based on a different resampling (also 10,000 iterations) of the same data. See Appendix C for equivalent graphs using peak forcing rather than eruption years.**

205 The results show a repeated coincidence between volcanic eruptions and famines, with famines occurring between 0 and 3 years after many major volcanic events. Regionally, these effects are concentrated in north China in the year of an eruption; in central China one, two and three years following an eruption, with a strong peak three years after; and in the far south of China one year following an eruption. The same methodology was used to produce SEA plots for extreme El Niño/La Niña



210 years (see Appendix D). These indicate that the temporal association between ENSO extremes and famine in China is weaker and less consistent than that observed for volcanic eruptions, although results vary depending on the reconstruction used. The only exception is in northern China, where famines peak significantly one year before a major El Niño event.

To break down the possible causal links between famine and volcanic eruptions, we can also examine SEAs showing how summer temperature, drought occurrence, crop failure and flooding correspond to major eruptions (Fig. 5).



215

**Figure 5. Superposed epoch analysis showing summer temperature (STI), drought (DI) and crop failure (CFI) indices, relative to eruption years, for the three study regions. Purple, yellow and red lines show the mean and 95% confidence band for the Monte Carlo resampling (10,000 iterations). Note that the p values are based on a different resampling (also 10,000 iterations) of the same data. See Appendix E for equivalent graphs showing flood index (FI) data.**

220

The SEA shows that while major eruptions do coincide with low temperatures, drought and crop failure, temporal patterns are highly regionally specific. Consistent summer temperature changes occur only in north and central China in years 0 and 1 following an eruption. Significant post-eruption droughts occur in central China (but nowhere else) in years 2 and 4, and crop failures spike in years 1, 3 and 3 in south, central and north China respectively. The most significant change is the major spike in crop failures in central China, year 3, which seems to correspond to a similar spike in famine occurrence (see Fig. 4).

225



Equivalent graphs for flooding (see Appendix E) show no significant connection to volcanic eruptions. Note that both north and central eastern China show significant temperature peaks before eruptions, a reminder that SEA plots indicate coincidence, not causality.

230 We can also examine the effects of ENSO on the same climate and environmental indices (Appendix F). A summary of the statistically significant results is shown in Table 3.

235 **Table 3. Statistically significant SEA results for Zhu et al. (2022) extreme El Niño/La Niña events (see Table 2). Showing results for summer temperature (STI), drought (DI), flood (FI), crop failure (CFI) and famine (FAI). See Appendix D and Appendix F for the full SEA results, including those for alternative ENSO reconstructions.**

Lag year	Extreme El Niño			Extreme La Niña		
	North Eastern China	Central Eastern China	South Eastern China	North Eastern China	Central Eastern China	South Eastern China
-5						
-4					Low STI High CFI	Low FI
-3	High FI					
-2				High DI	Low STI	
-1	High FAI		Low STI		Low STI	Low STI
0			High FI High CFI	High FI		
+1						
+2			High DI			
+3						Low STI
+4						
+5			High FI	High FI High CFI	High CFI	

240 These show both significant and consistent coincidence between extreme ENSO events and climate and agricultural disruption in eastern China. Of particular interest are the strong links between ENSO and flooding, which are absent from the volcanic eruption SEAs. However, the timing and strength of these associations vary considerably between reconstructions, making it hard to draw robust conclusions about the timing and magnitude of El Niño and La Niña impacts.

### 3.3 Correlations between climate, crops and famine

Next, we examine the more general correlations between the summer temperature, drought, flood, crop failure and famine indices in each of the three regions (Table 4).

245

**Table 4. Correlation coefficients between summer temperature (STI), drought (DI), flood (FI), crop failure (CFI) and famine (FAI) indices for the three study regions of China. The bottom and leftmost values use the Spearman’s Rank method, while the top and**

<https://doi.org/10.5194/egusphere-2026-1228>

Preprint. Discussion started: 8 April 2026

© Author(s) 2026. CC BY 4.0 License.



**right use the Pearson method. Correlation significance is denoted by asterisks: \*\*\* =  $p < 0.01$ ; \*\* =  $p < 0.05$ ; \* =  $p < 0.1$ . Where  $|r| < 0.1$  and  $p \geq 0.1$ , coefficients are replaced with a dash to indicate no significant correlation.**



**a**

<i>North Eastern China</i>	STI	DI	FI	CFI	FAI	
<b>STI</b>	1	-	-	-	-	Pearson
<b>DI</b>	-	1	-0.138***	0.630***	0.739***	
<b>FI</b>	-	-0.216***	1	0.326***	-	
<b>CFI</b>	-	0.387***	0.393***	1	0.632***	
<b>FAI</b>	-	0.527***	-	0.500***	1	
	Spearman					

**b**

<i>Central Eastern China</i>	STI	DI	FI	CFI	FAI	
<b>STI</b>	1	0.136***	-	-	-	Pearson
<b>DI</b>	0.161***	1	-0.129***	0.385***	0.591***	
<b>FI</b>	-0.103**	-0.106**	1	0.577***	0.156***	
<b>CFI</b>	-	0.334***	0.512***	1	0.497***	
<b>FAI</b>	-	0.461***	0.211***	0.510***	1	
	Spearman					

**c**

<i>South Eastern China</i>	STI	DI	FI	CFI	FAI	
<b>STI</b>	1	-	-	-0.112**	-	Pearson
<b>DI</b>	-	1	-0.100**	0.255***	0.383***	
<b>FI</b>	-	-	1	0.633***	0.119**	
<b>CFI</b>	-0.162***	0.276***	0.507***	1	0.235***	
<b>FAI</b>	-	0.410***	0.131***	0.293***	1	
	Spearman					

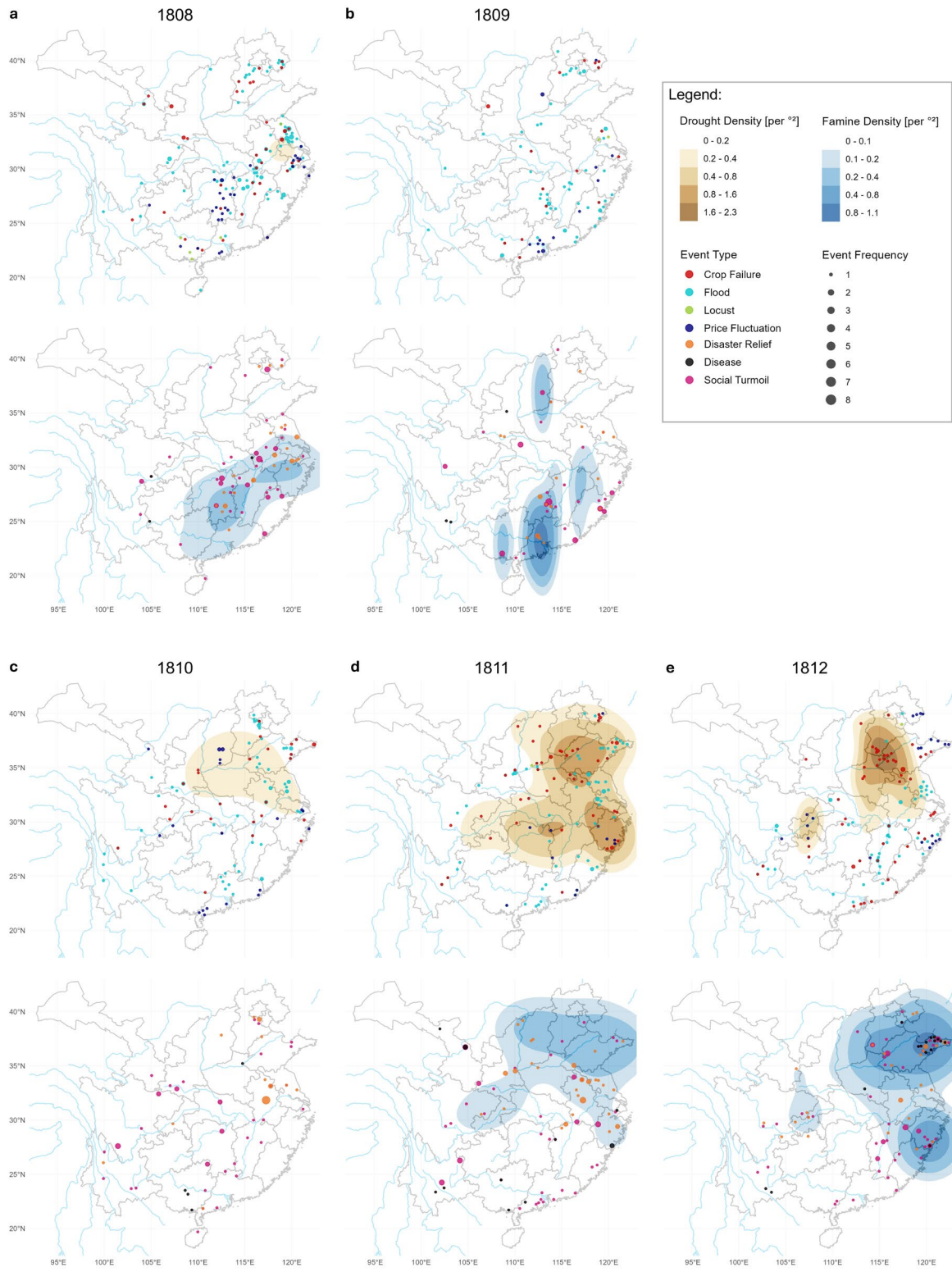


In all three regions, drought, crop failure and famine are significantly correlated with each other. Flood correlations are slightly more variable, and summer temperature is only significantly correlated with drought in central China and crop failure in southern China. Most of these relationships are approximately linear. Of the four other indices, drought correlates most strongly with famines in all three regions, with crop failure a close second. Interestingly, drought always correlates more strongly with famine than with crop failure, possibly indicating a separate process connecting drought to famines. The drought, crop failure, and famine correlations all seem to weaken as they move south, although the flood-crop failure correlations show the opposite trend, being much stronger in central and south eastern China than in the north east.

Evidence for a direct correlation between the REACHES indices and volcanic activity, as measured by SAOD (Toohey and Sigl, 2017), was assessed using lagged correlations to account for the delayed nature of volcanic impacts (see Appendix G). Across all regions,  $r$  values indicate at best very weak correlations, although some results are statistically significant. In northern China, volcanic eruptions are correlated with flooding and crop failure, and inversely correlated with summer temperature and drought, but this does not translate into any correlation with famines. Meanwhile in southern China there is little or no correlation between SAOD and climate, crops or famine. Only in the central China region do famines correlate with volcanic activity, which is also where we see the strongest correlations with crop failure.

### **3.4 Case Studies: The 1809 “Unknown” eruption and the eruptions of 1641, 1783 and 1815**

Having identified statistically significant coincidence between volcanic eruptions, drought, crop failure and famine (at least for central China), the remaining question is whether these relationships are causal. This can be addressed by examining individual eruptions in detail to trace the specific climatic and societal pathways through which they may have produced famine. To complement the existing literature, we have produced a short case study examining the impacts of the 1809 “unknown” eruption – the largest (as measured by SAOD) eruption in the Qing dynasty that has not been studied in detail.





275 **Figure 6. Point and kernel density plots showing the annual distribution of drought and famine reports, and the location and frequency of related events, 1808 to 1812. Note that owing to a larger overall number of reports in the REACHES database (see Fig. 2) droughts, famines and events in northeast China may be over-represented.**

The spatial plots from 1808 to 1812 (Fig. 6) show severe droughts in the vicinity of the Yellow (north-east) and Yangtze (central-east) rivers in 1811 and 1812, with the most extreme being in the north-east in 1812. These correspond to reported  
280 famines across north-east China in 1811, centred on Shandong province, that worsened and spread to central-east China (around Zhejiang province) in 1812. Before this, we can see famines of similar magnitude in south and central eastern China in 1809 and 1810 (the worst being in Guangdong province in 1810, near the mouth of the Pearl river), although these do not coincide with any major drought or flood. Isolated crop failures were reported throughout the period, only reaching a high density in 1811 and 1812 around the Yellow river in the north-east. In all years there are numerous flood records in different  
285 regions of China, but 1808, 1811 and 1812 seem to have been particularly bad flood years. Locust outbreaks do not appear to have been a major issue. Reports of social turmoil and disaster relief are widespread and seem only partially connected to the famines, although there was a major disease outbreak in eastern Shandong in 1812 which could well be linked to the 1811-1812 famine there. Possibly the most interesting events are the reports of major price fluctuations, which often (though not always) seem to correspond with regions of famine – for example in the south of Zhejiang province in 1812 where we see  
290 famine and a cluster of price fluctuations, but minimal incidence of drought, crop failure or flooding.

A summary of these results, combined those from three additional case studies from the 1440 to 1900 period (Gao et al., 2017; Chen et al., 2020; Gao et al., 2021b) is presented in Table 5.

295 **Table 5. Summary of four case studies that examined the climate, environmental and social impacts of volcanic eruptions in 1641, 1783, 1809 and 1815. Note that Yrs 0, 1, 2 and 3 refer to the year of an eruption and the first, second and third year following.**



Erupcion	Pre-eruption Conditions	Volcano/Climate Mechanisms	Climate Response	Environmental Impacts	Social Impacts	Famine Outcomes
<b>Parker, 1641</b> (Chen et al. 2020)	<ul style="list-style-type: none"> <li>Ongoing drought (<i>natural variability</i>), strongest in north China</li> <li>Political corruption, peasant uprisings, border crises</li> </ul>	<ul style="list-style-type: none"> <li>Reduced land–sea temperature gradient weakens EASM*</li> <li>WPSH** weakens and moves eastwards, weakening EASM</li> <li>Soil-moisture feedbacks reduce precipitation (Yr 1-3)</li> </ul>	<ul style="list-style-type: none"> <li>Volcanic cooling</li> <li>Prolonged and worsened drought</li> <li>Drought expands into southern China (Yr 0)</li> </ul>	N/A	<ul style="list-style-type: none"> <li>Disease outbreaks</li> <li>Social unrest, political instability and dynastic collapse</li> </ul>	<ul style="list-style-type: none"> <li>Widespread famine and mortality</li> </ul>
<b>Laki, 1783</b> (Gao et al. 2021b)	<ul style="list-style-type: none"> <li>Population growth and political corruption, leaving people vulnerable to subsistence crises</li> </ul>	<ul style="list-style-type: none"> <li>Different in aerosol forcing in N and S hemispheres shifts ITCZ*** southwards, suppressing rainfall</li> <li>(Possibly volcanic) El Niño causes wetting in north and central eastern China (Yr 0-1)</li> <li>La Niña reinforces drying caused by the eruption (Yr 2)</li> </ul>	<ul style="list-style-type: none"> <li>Severe drought in north eastern China (Yr 1) spreading to central (Yr 2) and south eastern China (Yr 3),</li> <li>Drying of rivers, lakes and ports (Yr 2-3)</li> </ul>	<ul style="list-style-type: none"> <li>Drought-triggered locust outbreaks (Yr 1-3)</li> <li>Drought-associated harvest failure</li> </ul>	<ul style="list-style-type: none"> <li>Price spikes related to bad harvests</li> <li>Famine-associated disease outbreaks (Yr 1-3, worst in Yr 3)</li> </ul>	<ul style="list-style-type: none"> <li>Worsening famine across eastern China (Yr 1-3, peaking in Yr 3)</li> <li>Reports of cannibalism</li> </ul>
<b>Unknown 1809</b>	<ul style="list-style-type: none"> <li>Famine in central and south eastern China</li> <li>Reduced STI across eastern China (1808)</li> </ul>	N/A	<ul style="list-style-type: none"> <li>Low STI in north and central eastern China (Yr 0)</li> <li>Worsening drought in north and central eastern China (Yr 1-3, peaking in Yr 3)</li> </ul>	<ul style="list-style-type: none"> <li>Drought-associated crop failures in north and central eastern China (Yr 2-3)</li> </ul>	<ul style="list-style-type: none"> <li>Price fluctuations associated with famines, but not crop failure or droughts (1808, Yr 0 and Yr 3)</li> <li>Famine-associated disease outbreak in north eastern China (Yr 3)</li> </ul>	<ul style="list-style-type: none"> <li>Famine in central and south eastern China (Yr 0 - likely a continuation preceding famine)</li> <li>Delayed famine in north and central eastern China (Yr 2 and Yr 3)</li> </ul>
<b>Tambora 1815</b> (Gao et al. 2017)	<ul style="list-style-type: none"> <li>Low summer temperatures</li> <li>Drought and famine in north and central eastern China</li> </ul>	<ul style="list-style-type: none"> <li>Aerosol-induced cooling (Yr 0-2)</li> <li>Reduced evaporation and cloud cover</li> <li>Reduced land–sea temperature gradient</li> </ul>	<ul style="list-style-type: none"> <li>Reduced summer temperatures (Yr 0-3, peaking in year 3)</li> <li>Frost and snow across south eastern China (Yr 0-1)</li> <li>Possible drought in central (Yr 1) and north (Yr 2) eastern China</li> </ul>	<ul style="list-style-type: none"> <li>Frost damage to crops and death of livestock from cold in central and southern China (Yr 0-1)</li> </ul>	<ul style="list-style-type: none"> <li>Plague leading to crops left unharvested in north eastern China (Yr 0)</li> </ul>	<ul style="list-style-type: none"> <li>Extreme famine in Yunnan province, south-central China (Yr 0-2) linked to cold growing seasons</li> <li>Some mild famines reported in other eastern provinces</li> </ul>

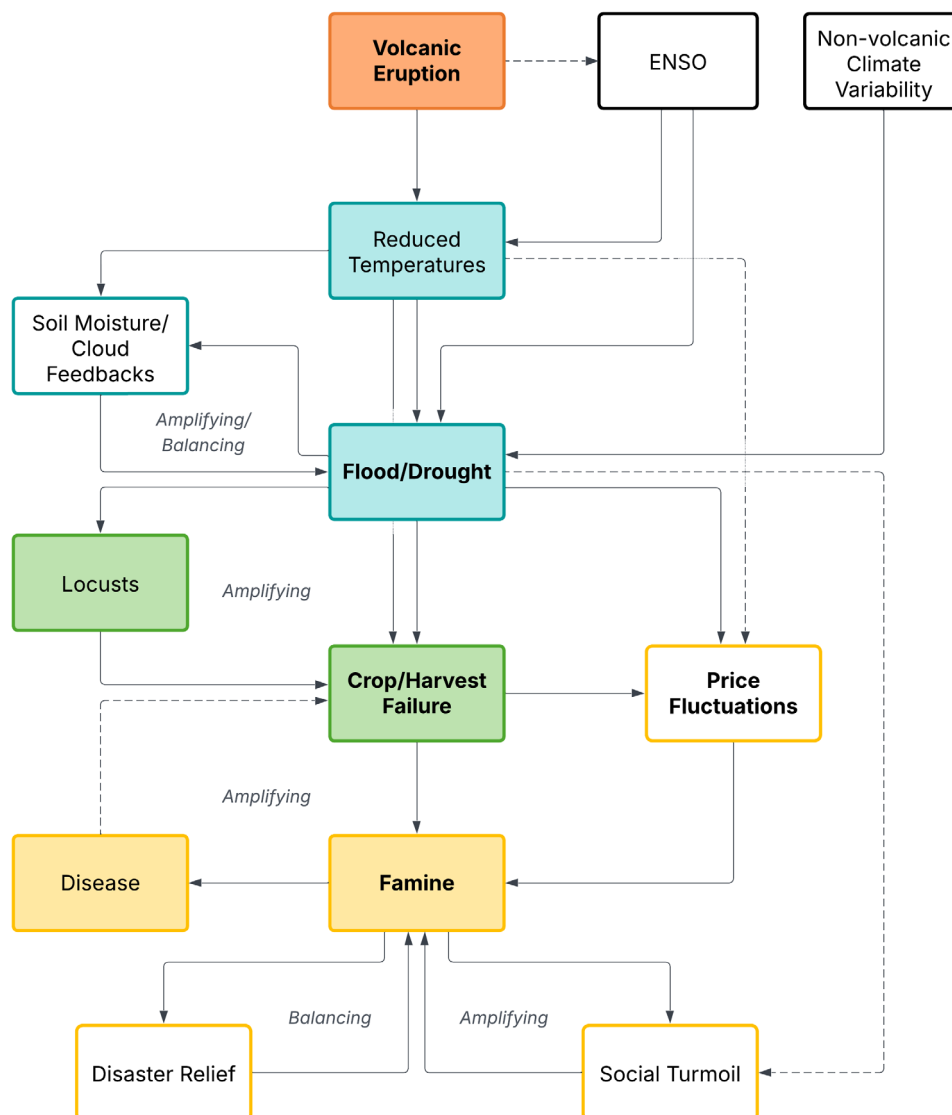
\*East Asian Summer Monsoon; \*\*Western Pacific Subtropical High; \*\*\*Intertropical Convergence Zone.



## 4 Discussion

### 300 4.1 Case studies and causality

The results presented above show repeated links between volcanic activity, drought and famine in eastern China, based on thirteen eruptions between 1440 and 1900. Drawing from the wider literature and the case studies (Table 5), this section examines how major eruptions contribute to famines, and how other factors moderate this relationship.



305 **Figure 7. Systems diagram showing the complex processes linking volcanic eruptions to famine in China. Feedback loops are identified as either amplifying or balancing, depending on whether they intensify or counteract existing trends. Weak or inferred causal connections are shown as dashed lines. The colour scheme follows the broad categories from Fig. 1.**



Figure 7 illustrates the general progression from post-volcanic cooling to increased incidence of flooding and drought, reduced  
310 crop production, rising food prices, and a greater risk of famine. However, it emphasises that at each stage there are other  
processes that can amplify or balance these changes. While many of the connections in the diagram are well-evidenced from  
both our results and the case studies, a few require further explanation. The connections between ENSO and  
temperature/flood/drought were apparent from both the SEA results and Gao et al. (2021b), but it should be noted that El  
Niño/La Niña cycles can both strengthen or counteract the effects of a volcanic eruption, and they rarely result in famine on  
315 their own. In contrast, non-volcanic climate variability is more than capable of causing famine (see Table 4). It can also  
determine volcanic impacts both on climate (through the superposition of volcanic and non-volcanic effects) and society  
(through its effects on the period preceding an eruption). Lin et al. (2020), Gao et al. (2021b) and Yang and Ludlow (2025)  
highlight locusts as an occasional but important factor determining how droughts translate into crop failures. Drought creates  
ideal breeding conditions for locusts (Lin et al., 2020), meaning that outbreaks may be more likely following a volcanic  
320 eruption. The relative importance of food prices requires further investigation, as the REACHES database only records the  
general category of “Price Fluctuations”. Based on Sen (1982) and Yang and Ludlow (2025) it seems likely that both crop  
failure and anticipated crop failure (due to cold temperatures or a delayed monsoon, for example) could drive up food prices  
and lead to famine amongst the poor. The link from flood and drought (and indeed crop/harvest failure could also be connected  
here) to social turmoil is based on Gao et al. (2021a), where it is mentioned that such natural disasters could weaken the  
325 mandate of the Emperor and the Imperial bureaucracy, thus leading to popular unrest.

The limitations of this diagram should also be acknowledged. It is generalised over the whole of China, yet volcanic impacts  
vary considerably between eruptions and regions. Many of the mechanisms linking volcanic eruptions, temperature and  
hydroclimate are not included, although these are summarised in the introduction and case studies. Several important economic  
330 and social factors were also excluded, since they lacked sufficient evidence in REACHES or the case studies. Trade, market  
integration and grain imports/exports were all significant to the transmission of and relief from the impacts of natural disasters  
- and varied greatly between provinces, regions and time periods (Li, 2007). Food transportation may also have been impacted  
when extreme droughts caused the drying of river ports, such as after the Laki (1783) eruption. Access to state relief -  
sometimes directed by the emperor himself during times of crisis - was similarly important, but again varied across regions,  
335 time periods and imperial administrations (Marks, 1998; Li, 2007). Over the Qing dynasty, the granary relief system, which  
formed the backbone of such aid, became increasingly tied to market systems, as administrators came to rely on purchasing  
grain in times of famine, rather than on local storage (Marks, 1998). This shift created a feedback loop that linked famine relief  
to fluctuating grain prices. Migration represents another complex factor that could either alleviate or exacerbate famine  
conditions: populations might move towards areas of higher food production or better access to aid, but such movements could  
340 also increase mortality through crowding and the spread of disease (Sen, 1982; Pankenier, 2022; Warren, 2026).



## 4.2 Volcanic impacts on the different regions of China

Despite these shortcomings, by combining the processes from Fig. 7 with the SEA and correlation results, we can now both summarise and begin to explain the impacts of volcanic eruptions on the three main study regions. Across China, there seems to be a double peak in famines following volcanic eruptions – one immediate, and one delayed (see Fig. 4a and Appendix C).  
345 This suggests that both immediate cooling and hydroclimate disruption in years 0 and 1 can trigger famine, as can the slower-acting climatological and social feedback loops set in motion by the eruption (Fig. 7).

In north eastern China, low summer temperatures (Fig. 5a; Table G1a) and the potential for drought (Fig. 5b; Tambora, 1815) and flooding (Table G1a; Laki, 1783) in year 0 to 1 following an eruption, are associated with only minor crop failures (Fig. 350 5c; Table G1a). However, the climatic disruption may cause a failure of confidence in the harvest, leading to potential price spikes and increase in famine incidence (Fig. 4b), as observed in 1809 (Fig. 6b). The cause of crop failures in year 3 (Fig. 5c) is less clear, but may be the increased, though not statistically significant, prevalence of drought in the preceding years (Fig. 5b; Unknown, 1809). The case studies and volcano-climate literature suggest that the inconsistent volcanic impacts on north-eastern China might partly be due variable hydroclimatic impacts: eruptions sometimes causing drought, but also occasionally 355 having the reverse effect. It is also possible that a greater reliance on wheat agriculture (Yin et al., 2024) and proximity and access to direct relief from the emperor and central government in Beijing made north eastern China more resilient to longer-term climatic stress than other regions.

In central China, low temperatures in years 0 to 1 following an eruption (Fig. 5d; Table G1b) may have caused some crop 360 failures (Table G1b), leading to an increased famine occurrence in years 1 and 2 (Fig. 4b), as observed after Tambora in 1815/16. By year 2, temperatures have returned to normal, but significant drought kicks in (Fig. 5e), producing a spike in crop failures (Fig. 5f) and a corresponding spike in famine in year 3 (Fig. 4b). We see this central China-drought effect in all four case studies. The delayed impact likely reflects the counteracting influence of concurrent El Niños (Gao et al., 2021b; Liu et al., 2022) and the time required for the different amplifying processes in Fig. 7 to take effect. North-south variation in the 365 boundary between post-eruption wetting and drying (Gao and Gao, 2018; Gao et al., 2021b) may also reduce the consistency of any such drought responses.

In the south of China, the climatic impacts of eruptions are highly inconsistent. In particular, there is no clear or consistent cooling effect (Fig. 5g; Table G1c), although that may be an artifact of limited variability in the STI for south eastern China 370 (see Fig. 4e). The lack of significant hydroclimate impacts is broadly consistent with the literature (Gao and Gao, 2018; Liu et al., 2022; Zhuo et al., 2023), in which south eastern China tends to see less extreme changes than the rest of China. Increased crop failures in the first year following an eruption (Fig. 5i) may therefore be due to reduced temperatures (see Tambora, 1815)



or increased flood occurrence (Table 4c) but this remains highly speculative. These crop failures do appear to result in famines in the same year however (Fig. 4c), suggesting a very direct connection from crop failure to famine in southern China.

### 375 4.3 Further considerations and research

We have already identified some of the missing elements from our causal explanation of volcanic impacts on China, but a few further considerations should be included here. The first, as alluded to in the previous section, is agriculture. Staple crops vary between the study regions: rice is grown across south eastern China and much of central eastern China, while wheat is more prevalent in the north east and the north of central eastern China (Yin et al., 2024). Cropping intensity also differs, with some  
380 regions relying on a single annual harvest (north eastern China and the north of central eastern China), whereas others support double or even triple cropping (south eastern China and the south-central eastern China; (Tian et al., 2015). These systems respond differently climatic stress. Wheat is generally more resistant to adverse conditions, while rice is highly sensitive both drought and cold (Tian et al., 2015; Yin et al., 2024). Multiple cropping meanwhile, may either amplify or buffer volcanic impacts: it can exacerbate subsistence shocks if drought, flood or cold persist throughout the year, or mitigate them if only part  
385 of the growing season is affected. The more marginal nature of rice agriculture in central eastern China (at the northern edge of rice's growing range) coupled with its importance as a staple crop could also explain that regions sensitivity to volcanic climate disturbance. A promising avenue for future research might be to use coupled climate-agricultural models to simulate how post-volcanic climatic disruption affects crop yields in different regions of China (Flückiger et al., 2017).

390 There are also sampling issues with our set of 13 major volcanic eruptions. Three coincide with extreme EL Niño/La Niña years, and four occur within six years of another major eruption – both factors that obscure the signal from a single volcanic event (see Gao et al., 2021b). Furthermore, as Zhuo et al. (2023) point out, eruption latitude and timing influence climate impacts. Since our sample comprises three northern hemisphere eruptions and ten tropical eruptions, we can say very little about the impact of southern hemisphere volcanic activity or the different effects of northern hemisphere and tropical eruptions.  
395 Expanding the number of case studies – particularly for northern hemisphere eruptions - or extending our data sources further back in time would give a larger sample of eruptions for comparison. It would also allow the removal of closely spaced eruptions from the sample and more detailed investigation of eruption impacts under different of ENSO phases.

While we have offered a general causal explanation and summary of regional volcanic impacts across China, more granular  
400 analysis is clearly required explain famine dynamics in detail. We have already mentioned some of the broad factors missing from our framework, but there are almost certainly others that are specific to individual eruptions, time periods or geographical areas. Future studies could investigate the roles of famine relief, migration, trade networks, market integration, and price volatility at provincial, prefectural, or county scales. Detailed grain price data could be especially valuable - extending beyond the simple price fluctuations recorded in REACHES – allowing direct comparison of market prices with drought, flood and  
405 summer temperature indices. This could be used to assess our hypothesis for a direct connection between



temperature/hydroclimate and prices. Further case studies could also assess whether our regional SEAs, correlations and causal explanations are consistent with other eruptions and at finer spatial scales.

## 5 Conclusions

This study provides a multi-regional synthesis of volcanic impacts on famine across a large sweep of Chinese history (from 1440 to 1900). Scatterplots and correlation analysis based on the REACHES database confirm that volcanic climate disruption is not the main cause of famine in China. However, SEA reveals that famine occurrence and severity do increase significantly across northern, central and southeastern China following major eruptions. The timing and intensity of post-eruption famines varies considerably between eruptions and regions, with the most severe famines in northern China in the year of an eruption, in central China in the third year following and in southern China in the first year following. The co-occurrence of famines and volcanic activity is consistent with the expected effects of climatic disruption following a major volcanic event, where cooling, drought and floods can all contribute to subsistence crises. Such effects are evident from SEA and correlation results, which show reduced summer temperatures (year 0 and 1 post-eruption) and a delayed or prolonged drought response (years 1 to 4) across north and central eastern China. SEA of extreme ENSO years found significant associations with summer cooling, hydroclimate extremes, and agricultural disruption, but only minimal coincidence between El Niño/La Niña events and famine. However, uncertainties in dating past ENSO events suggests that SEA may not be the most suitable method for reconstructing such impacts.

Crop failure appears to be the principal mechanism linking volcanic climatic shocks to famine, although case studies from specific eruptions suggest that price speculation also plays a contributory role. A wide range of additional factors - including ENSO variability, non-volcanic climate variability, locust outbreaks, disease, famine relief, and social unrest - can amplify or counteract the impacts of an eruption. Many of these processes form feedback loops that shape the intensity and timing of volcanic effects: Soil moisture and cloud feedbacks may amplify or delay hydroclimatic responses, while the Chinese state relief system could sometimes counteract or postpone famine conditions. Given the spatial variability of volcanic climate effects - particularly shifts in wet-dry boundaries - it may be more appropriate to assess impacts in terms of a heightened risk of extremes rather than deterministic index responses. From this perspective, volcanic eruptions lead to:

1. Decreased summer temperatures; and
2. Increased likelihood of hydroclimate anomalies (drought and flooding).

These disruptions, in turn, elevate the risk of crop failure, locust outbreaks and price volatility, thereby increasing famine risk.

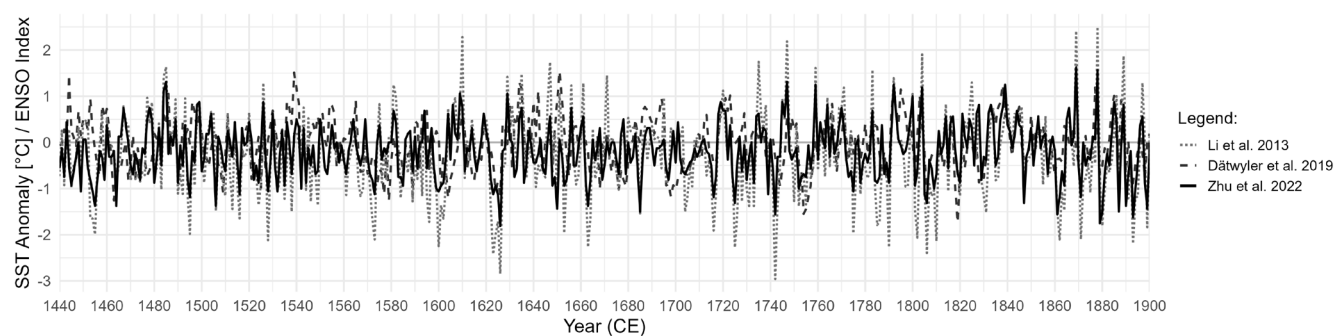
Our conclusions are necessarily constrained by our own timeframe (1440–1900), by the REACHES database, and by the focus on eastern China. While the causal mechanisms identified here likely extend further back in time, testing this would require additional historical datasets and eruption case studies. The extent to which these findings apply to contemporary China also



remains uncertain given profound changes in agriculture, infrastructure, markets, and governance since 1900. Nevertheless, the historical record demonstrates clearly that major volcanic eruptions — particularly when coupled with extreme hydroclimate variability — have the capacity to produce severe agricultural disruption and subsistence crises.

## Appendices

### Appendix A – Alternative ENSO reconstructions



445 **Fig. A1.** ENSO reconstructions, 1440-1900 CE. Showing Li et al. (2013) SST anomalies (dotted), Dätwyler et al. (2019) ENSO index (dashed) and Zhu et al. (2022) SST anomalies (solid). Note: Li et al. (2013) is based on a set of tree ring chronologies also used in Zhu et al. (2022), so the two data sets are not completely independent.

**Table A2.** Extreme El Niño and La Niña years between 1440 and 1900 CE, identified from Li et al. (2013) and Dätwyler et al. (2019).

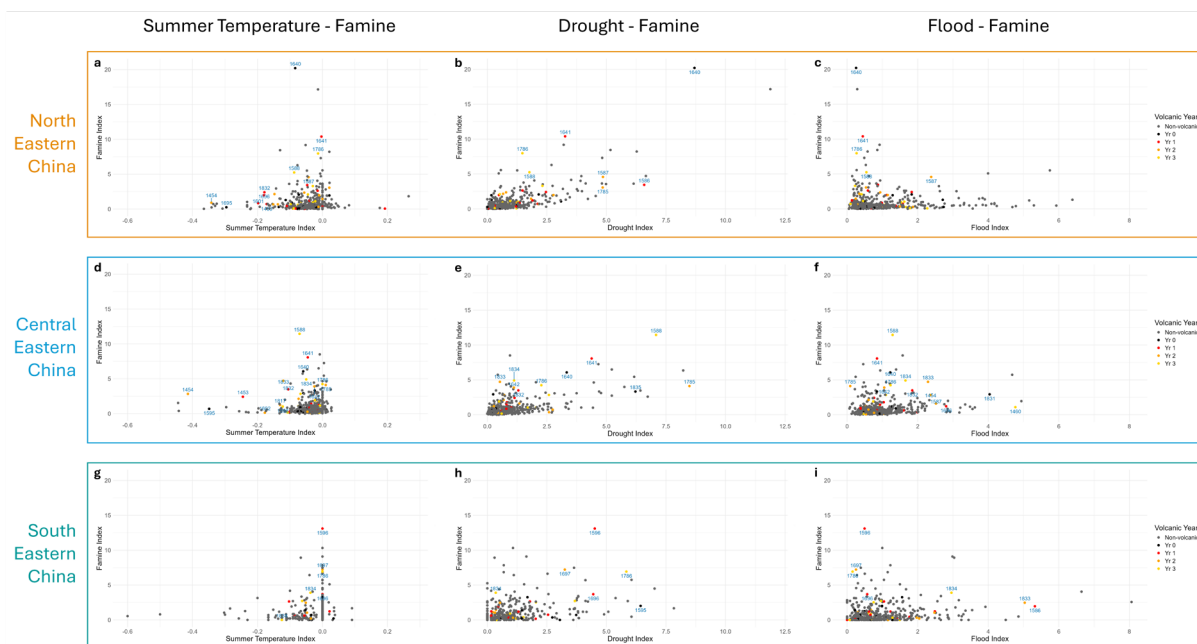


<i>Li et al. 2013</i>				<i>Dätwyler et al. 2019</i>			
<i>El Niño</i> <i>Years</i>	<i>SST</i> <i>Anomaly</i> <i>[°C]</i>	<i>La Niña</i> <i>Years</i>	<i>SST</i> <i>Anomaly</i> <i>[°C]</i>	<i>El Niño</i> <i>Years</i>	<i>ENSO</i> <i>Index</i>	<i>La Niña</i> <i>Years</i>	<i>ENSO</i> <i>Index</i>
-	-	<b>1455</b>	1.992	<b>1444</b>	0.29	-	-
<b>1485</b>	1.634	<b>1495</b>	1.984	<b>1453</b>	-1.634	<b>1463</b>	-0.254
<b>1526</b>	1.288	<b>1528</b>	2.119	<b>1486</b>	0.131	<b>1509</b>	-0.87
<b>1581</b>	1.247	<b>1573</b>	2.104	<b>1496</b>	-0.057	<b>1525</b>	-0.914
<b>1610</b>	2.280	<b>1600</b>	2.250	<b>1536</b>	-0.4	<b>1579</b>	0.126
<b>1629</b>	1.420	<b>1623</b>	2.419	<b>1539</b>	0.191	<b>1589</b>	-1.279
<b>1635</b>	1.487	<b>1626</b>	2.842	<b>1565</b>	0.324	<b>1601</b>	-1.363
<b>1647</b>	1.740	<b>1653</b>	1.964	<b>1634</b>	0.611	<b>1604</b>	0.739
<b>1656</b>	1.234	<b>1663</b>	2.266	<b>1642</b>	-0.5	<b>1626</b>	-2.842
<b>1661</b>	1.283	<b>1716</b>	1.909	<b>1651</b>	1.053	<b>1668</b>	0.192
<b>1671</b>	1.451	<b>1725</b>	2.273	<b>1694</b>	-0.561	<b>1676</b>	-1.025
<b>1735</b>	1.745	<b>1742</b>	2.962	<b>1723</b>	0.374	<b>1679</b>	-0.318
<b>1747</b>	2.191	<b>1775</b>	1.972	<b>1792</b>	1.395	<b>1698</b>	0.304
<b>1759</b>	1.613	<b>1785</b>	1.788	<b>1795</b>	0.069	<b>1744</b>	-0.547
<b>1771</b>	1.188	<b>1790</b>	2.271	<b>1803</b>	-0.074	<b>1754</b>	-0.726
<b>1783</b>	1.573	<b>1802</b>	2.062	<b>1838</b>	0.238	<b>1806</b>	-2.394
<b>1792</b>	1.395	<b>1806</b>	2.394	<b>1877</b>	-0.453	<b>1819</b>	-0.58
<b>1804</b>	1.906	<b>1810</b>	2.136	<b>1885</b>	0.191	-	-
<b>1825</b>	1.297	<b>1862</b>	2.104	<b>1888</b>	0.109	-	-
<b>1869</b>	2.413	<b>1871</b>	2.095	-	-	-	-
<b>1878</b>	2.504	<b>1880</b>	1.809	-	-	-	-
<b>1889</b>	1.872	<b>1893</b>	2.193	-	-	-	-
<b>1897*</b>	1.288	<b>1899*</b>	1.838	-	-	-	-

450 \*These years were excluded from the SEA, as the event year + 5 was outside of our data range. Underlined years are those that match extreme El Niño and La Niña years identified from the Zhu et al. (2022) reconstruction (see Table 2).



## Appendix B – Further index comparison



455 **Fig. B1.** Scatterplots showing the distribution of STI, DI, FI and FAI in north, central and south eastern China for volcanic and non-volcanic years. Labeled points are the years following major eruptions that are also in the top 5% of years in either index.



### Appendix C - Peak volcanic forcing year-famine SEAs

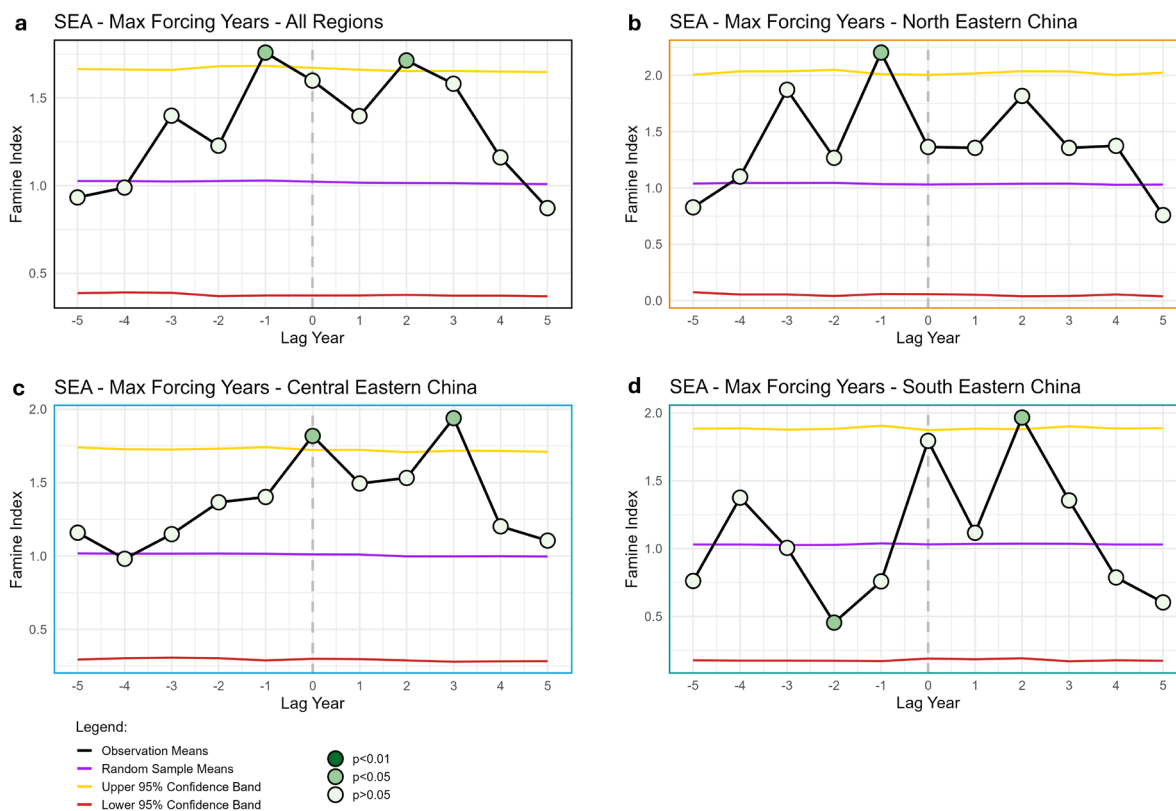
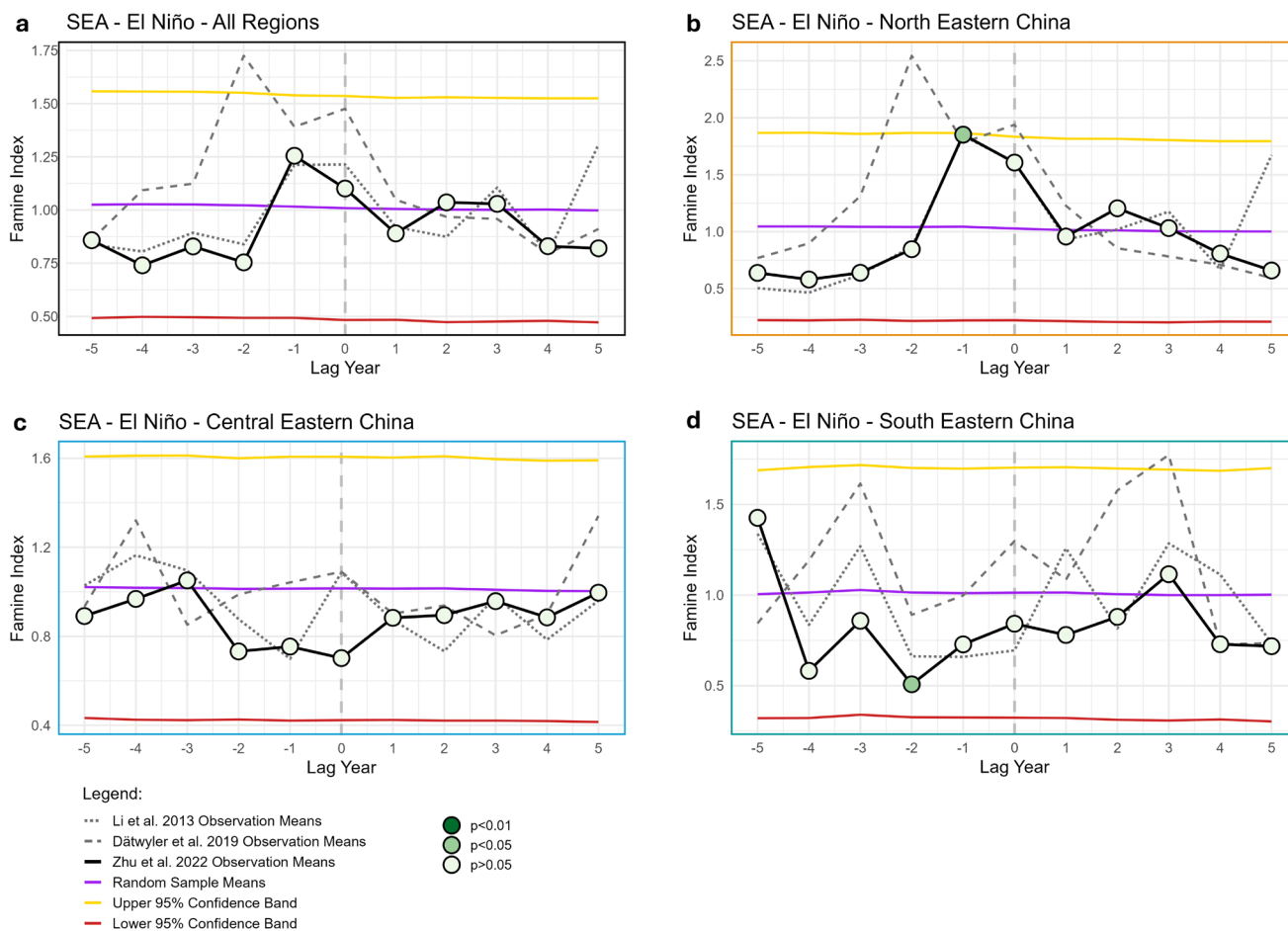


Fig. C1. Superposed epoch analysis showing famine index (FAI), relative to peak forcing years, for the three study regions. Purple, yellow and red lines show the mean and 95% confidence band for the Monte Carlo resampling (10,000 iterations). Note that the p values are based on a different resampling (also 10,000 iterations) of the same data.

460



### Appendix D – Extreme ENSO-famine SEAs



**Fig. D1.** Superposed epoch analysis showing famine index (FAI), relative to extreme El Niño years, for the three study regions. Purple, yellow and red lines show the mean and 95% confidence band for the Monte Carlo resampling (10,000 iterations). Note that the p values are based on a different resampling (also 10,000 iterations) of the same data.

465

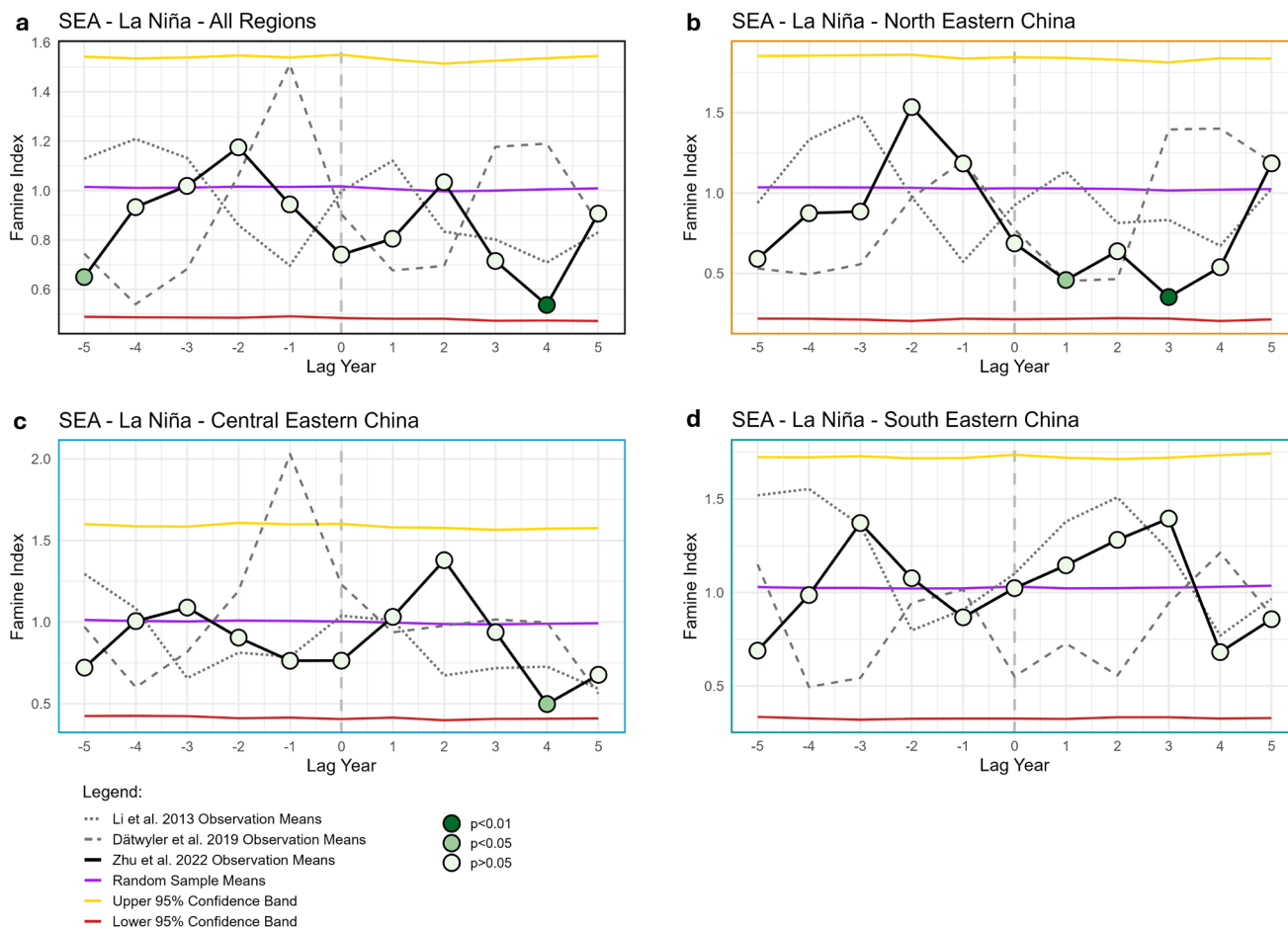


**Fig. D2.** Superposed epoch analysis showing famine index (FAI), relative to extreme La Niña years for the three study regions. Purple, yellow and red lines show the mean and 95% confidence band for the Monte Carlo resampling (10,000 iterations). Note that the p values are based on a different resampling (also 10,000 iterations) of the same data.



470 Appendix E – Eruption-flood SEAs

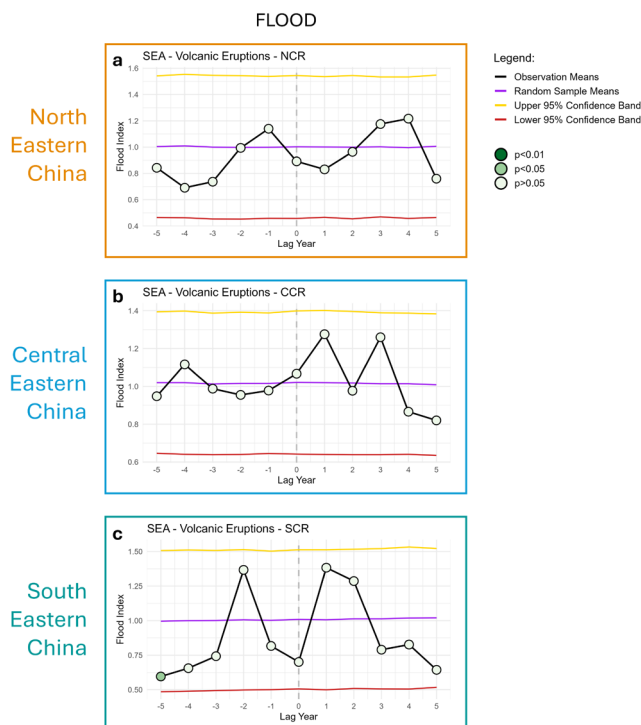


Fig. E1. Superposed epoch analysis showing flood index (FLI), relative to eruption years for the three study regions. Purple, yellow and red lines show the mean and 95% confidence band for the Monte Carlo resampling (10,000 iterations). Note that the p values are based on a different resampling (also 10,000 iterations) of the same data.



475 Appendix F - Extreme ENSO-temperature, drought, flood and crop failure SEAs

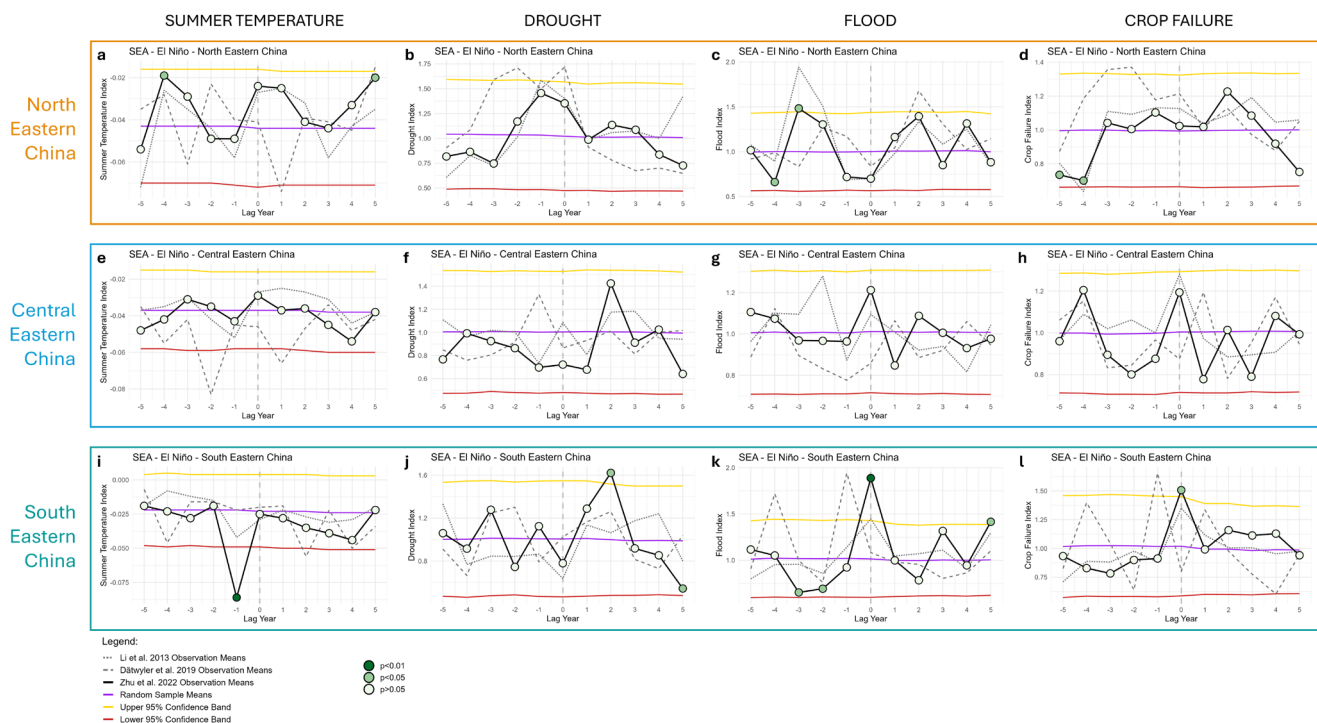
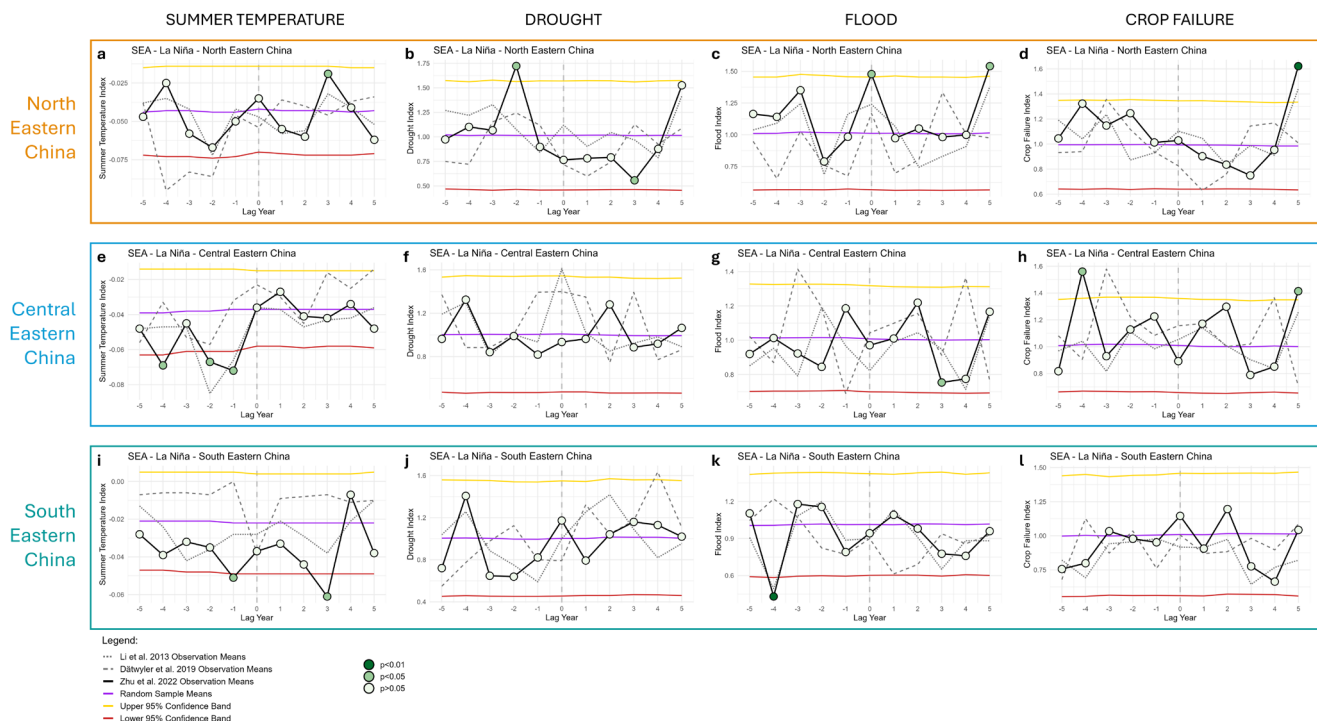


Fig. F1. Superposed epoch analysis showing summer temperature (STI), drought (DI), flood (FI) and crop failure (CFI) indices, relative to extreme El Niño years, for the three study regions. Purple, yellow and red lines show the mean and 95% confidence band for the Monte Carlo resampling (10,000 iterations). Note that the p values are based on a different resampling (also 10,000 iterations) of the same data.

480



**Fig. F2.** Superposed epoch analysis showing summer temperature (STI), drought (DI), flood (FI) and crop failure (CFI) indices, relative to extreme La Niña years, for the three study regions. Purple, yellow and red lines show the mean and 95% confidence band for the Monte Carlo resampling (10,000 iterations). Note that the p values are based on a different resampling (also 10,000 iterations) of the same data.

485



### Appendix G – Lagged SAOD correlations

490

**Table G1. Lagged correlation coefficients between SAOD and summer temperature (STI), drought (DI), flood (FI), crop failure (CFI), famine (FAI) indices for the three study regions of China. Correlation method is denoted by black (Pearson) and grey (Spearman) text. Correlation significance is denoted by asterisks: \*\*\* =  $p < 0.01$ ; \*\* =  $p < 0.05$ ; \* =  $p < 0.1$ . Where  $|r| < 0.1$  and  $p \geq 0.1$ , coefficients are replaced with a dash to indicate no significant correlation.**

**a**

<i>North Eastern China</i>	SAOD (lag 0 year)	SAOD (lag 1 year)	SAOD (lag 2 year)	SAOD (lag 3 year)
<b>STI</b>	-0.124*** -0.141***	-0.156*** -0.100**	- -	- -
<b>DI</b>	- -	- -	- -0.090*	- -0.122***
<b>FI</b>	- 0.130***	- 0.098**	- 0.094**	- 0.095**
<b>CFI</b>	- 0.130***	0.110** -	0.097** -	- -
<b>FAI</b>	- -	- -	- -	- -

**b**

<i>Central Eastern China</i>	SAOD (lag 0 year)	SAOD (lag 1 year)	SAOD (lag 2 year)	SAOD (lag 3 year)
<b>STI</b>	-0.081* -0.084*	-0.081* -	- -	- 0.093**
<b>DI</b>	- -	- -	- -	- -
<b>FI</b>	- -	- -	- -	- -
<b>CFI</b>	- -	0.158*** -	0.194*** -	- -
<b>FAI</b>	0.105** -	0.077* 0.083*	0.081* 0.080*	- -

**c**

<i>South Eastern China</i>	SAOD (lag 0 year)	SAOD (lag 1 year)	SAOD (lag 2 year)	SAOD (lag 3 year)
<b>STI</b>	- -	- -	- -	- 0.082*
<b>DI</b>	- -	- -	- -	- -
<b>FI</b>	- -	- -	- -	- -
<b>CFI</b>	- -	- -	- -	- -
<b>FAI</b>	- -	- -	0.082* -	- -



### Code availability

495 All graphs were produced using the ggplot2 R package ([10.32614/CRAN.package.ggplot2](https://cran.r-project.org/web/packages/ggplot2/index.html)), while data and calculations were produced/conducted using the publicly available R packages cited in the text.

### Data availability

The REACHES database is available online via the NOAA repository at <https://www.ncei.noaa.gov/access/paleo-search/study/23410>.

500

The derived index data used for this study is publicly available at <https://boris-portal.unibe.ch/entities/product/d336e807-8c36-483c-a228-8817cd92ef6d>.

### Competing interests

The author declares that they have no conflict of interest.

505

### Acknowledgements

Kuan-Hui Elaine Lin (National Taiwan Normal University) – introduction to and assistance with using the REACHES database.

Heli Huhtamaa (University of Bern) and Martin Warren – scientific input and proof reading.

510 Zhen Yang (University of Bern) - historical input.

AI software (ChatGPT) was used for proofreading parts of this paper.

### Financial support

RW is supported by the Swiss State Secretariat for Education, Research and Innovation (contract number MB22.00030) and

515 Swiss National Science Foundation (grant number PZ00P1\_201953).



## References

- Brönnimann, S. and Krämer, D.: Tambora and the “Year Without a Summer” of 1816. A Perspective on Earth and Human Systems Science, *Geographica Bernensia*, G90, 1–48, <https://doi.org/10.4480/GB2016.G90.02>, 2016.
- Bunn, A., Korpela, M., Biondi, F., Campelo, F., Klesse, S., Mérian, P., Qeadan, F., and Zang, C.: dplR: Dendrochronology Program Library in R, version 1.7.8, 2025.
- 520 Büntgen, U., Di Cosmo, N., Esper, J., Frachetti, M., Khalidi, L., Mauelshagen, F., Rohland, E., and Oppenheimer, C.: Volcanoes, Climate, and Society, *Annual Review of Earth and Planetary Sciences*, <https://doi.org/10.1146/annurev-earth-032524-013254>, 2025.
- Burke, A., Innes, H. M., Crick, L., Anchukaitis, K. J., Byrne, M. P., Hutchison, W., McConnell, J. R., Moore, K. A., Rae, J. W. B., Sigl, M., and Wilson, R.: High sensitivity of summer temperatures to stratospheric sulfur loading from volcanoes in the Northern Hemisphere, *Proc. Natl. Acad. Sci. U.S.A.*, 120, <https://doi.org/10.1073/pnas.2221810120>, 2023.
- 525 Chen, K., Ning, L., Liu, Z., Liu, J., Yan, M., Sun, W., Yuan, L., Lv, G., Li, L., Jin, C., and Shi, Z.: One Drought and One Volcanic Eruption Influenced the History of China: The Late Ming Dynasty Mega-drought, *Geophysical Research Letters*, 47, <https://doi.org/10.1029/2020GL088124>, 2020.
- 530 Dätwyler, C., Abram, N. J., Grosjean, M., Wahl, E. R., and Neukom, R.: El Niño–Southern Oscillation variability, teleconnection changes and responses to large volcanic eruptions since AD 1000, *Intl Journal of Climatology*, 39, 2711–2724, <https://doi.org/10.1002/joc.5983>, 2019.
- Feng, X., Liu, D., Zhao, J., Si, W., and Fan, S.: Impact of climate change on farmers’ crop production in China: a panel Ricardian analysis, *Humanit Soc Sci Commun*, 12, <https://doi.org/10.1057/s41599-024-04287-5>, 2025.
- 535 Flückiger, S., Brönnimann, S., Holzkämper, A., Fuhrer, J., Krämer, D., Pfister, C., and Rohr, C.: Simulating crop yield losses in Switzerland for historical and present Tambora climate scenarios, *Environ. Res. Lett.*, 12, 74026, <https://doi.org/10.1088/1748-9326/aa7246>, 2017.
- Gao, C. C. and Gao, Y. J.: Revisited Asian Monsoon Hydroclimate Response to Volcanic Eruptions, *JGR Atmospheres*, 123, 7883–7896, <https://doi.org/10.1029/2017JD027907>, 2018.
- 540 Gao, C., Ludlow, F., Matthews, J. A., Stine, A. R., Robock, A., Pan, Y., Breen, R., Nolan, B., and Sigl, M.: Volcanic climate impacts can act as ultimate and proximate causes of Chinese dynastic collapse, *Commun Earth Environ*, 2, <https://doi.org/10.1038/s43247-021-00284-7>, 2021a.
- Gao, C., Gao, Y., Zhang, Q., and Shi, C.: Climatic aftermath of the 1815 Tambora eruption in China, *J Meteorol Res*, 31, 28–38, <https://doi.org/10.1007/s13351-017-6091-9>, 2017.
- 545 Gao, C.-C., Yang, L.-S., and Liu, F.: Hydroclimatic anomalies in China during the post-Laki years and the role of concurring El Niño, *Advances in Climate Change Research*, 12, 187–198, <https://doi.org/10.1016/j.accre.2021.03.006>, 2021b.
- Hao, Z., Xiong, D., Zheng, J., Yang, L. E., and Ge, Q.: Volcanic eruptions, successive poor harvests and social resilience over southwest China during the 18–19th century, *Environ. Res. Lett.*, 15, 105011, <https://doi.org/10.1088/1748-9326/abb159>, 2020.
- 550 Huhtamaa, H., Stoffel, M., and Corona, C.: Recession or resilience? Long-range socioeconomic consequences of the 17th century volcanic eruptions in northern Fennoscandia, *Clim. Past*, 18, 2077–2092, <https://doi.org/10.5194/cp-18-2077-2022>, 2022.
- Hutchison, W., Sugden, P., Burke, A., Abbott, P., Ponomareva, V. V., Dirksen, O., Portnyagin, M. V., MacInnes, B., Bourgeois, J., Fitzhugh, B., Verkerk, M., Aubry, T. J., Engwell, S. L., Svensson, A., Chellman, N. J., McConnell, J. R., Davies, S., Sigl, M., and Plunkett, G.: The 1831 CE mystery eruption identified as Zavaritskii caldera, Simushir Island (Kurils), *Proceedings of the National Academy of Sciences of the United States of America*, 122, e2416699122, <https://doi.org/10.1073/pnas.2416699122>, 2025.
- 555 Kim, S. W.: Two severe famines (1809–1810, 1814–1815) in Korea during the last stage of the Little Ice Age, *Clim. Past*, 21, 1521–1531, <https://doi.org/10.5194/cp-21-1521-2025>, 2025.



- 560 Li, H., Wang, X., Wang, S., Liu, J., Liu, Y., Liu, Z., Chen, S., Wang, Q., Zhu, T., Wang, L., and Wang, L.: ChinaRiceCalendar – seasonal crop calendars for early-, middle-, and late-season rice in China, *Earth Syst. Sci. Data*, 16, 1689–1701, <https://doi.org/10.5194/essd-16-1689-2024>, 2024.
- Li, J., Xie, S.-P., Cook, E. R., Morales, M. S., Christie, D. A., Johnson, N. C., Chen, F., D'Arrigo, R., Fowler, A. M., Gou, X., and Fang, K.: El Niño modulations over the past seven centuries, *Nature Clim Change*, 3, 822–826, <https://doi.org/10.1038/nclimate1936>, 2013.
- 565 Li, L. M.: *Fighting famine in North China: State, Market, and Environmental Decline, 1690s-1990s*, Stanford University Press, Stanford, California, 2007.
- Li, Y., Strapasson, A., and Rojas, O.: Assessment of El Niño and La Niña impacts on China: Enhancing the Early Warning System on Food and Agriculture, *Weather and Climate Extremes*, 27, 100208, <https://doi.org/10.1016/j.wace.2019.100208>, 2020.
- 570 Lin, K.-H. E., Wang, P. K., Pai, P.-L., Lin, Y.-S., and Wang, C.-W.: Historical droughts in the Qing dynasty (1644–1911) of China, *Clim. Past*, 16, 911–931, <https://doi.org/10.5194/cp-16-911-2020>, 2020.
- Liu, F., Gao, C., Chai, J., Robock, A., Wang, B., Li, J., Zhang, X., Huang, G., and Dong, W.: Tropical volcanism enhanced the East Asian summer monsoon during the last millennium, *Nature communications*, 13, 3429, <https://doi.org/10.1038/s41467-022-31108-7>, 2022.
- 575 Ljungqvist, F. C., Seim, A., and Huhtamaa, H.: Climate and society in European history, *WIREs Climate Change*, 12, <https://doi.org/10.1002/wcc.691>, 2021.
- Lv, A., Fan, L., and Zhang, W.: Impact of ENSO Events on Droughts in China, *Atmosphere*, 13, 1764, <https://doi.org/10.3390/atmos13111764>, 2022.
- 580 Marks, R.: *Tigers, Rice, Silk, and Silt: Environment and Economy in Late Imperial South China*, Cambridge University Press, 1998.
- Pankenier, D. W.: The climate downturns in China caused by volcanic eruptions in 535–40 CE and by Thera (Santorini) at the founding of the Shang dynasty (1562 BCE), *Asiatische Studien - Études Asiatiques*, 76, 763–784, <https://doi.org/10.1515/asia-2022-0042>, 2022.
- 585 Ripley, B. D., Venables, W. N., Bates, D. M., Hornik, K., Gebhardt, A., and Firth, D.: MASS: Support Functions and Datasets for Venables and Ripley's MASS, version 7.3-65, 2025.
- Ro, S., Hur, S. D., Ekaykin, A., Han, Y., Ro, C.-U., Hong, S.-B., Lee, M. J., Chang, C., Lee, S., Moon, J., Jung, H., Veres, A., Lee, A., and Hong, S.: Origin of the 1458/59 CE volcanic eruption revealed through analysis of glass shards in the firn core from Antarctic Vostok station, *Commun Earth Environ*, 6, <https://doi.org/10.1038/s43247-025-02797-x>, 2025.
- 590 Robock, A. and Mao, J.: The Volcanic Signal in Surface Temperature Observations, *J. Climate*, 8, 1086–1103, [https://doi.org/10.1175/1520-0442\(1995\)008<1086:TVSIST>2.0.CO;2](https://doi.org/10.1175/1520-0442(1995)008<1086:TVSIST>2.0.CO;2), 1995.
- Sen, A.: *Poverty and Famines: An Essay on Entitlement and Deprivation*, OUP Oxford, 1982.
- Tian, Z., Liang, Z., Sun, L., Zhong, H., Qiu, H., Fischer, G., and Zhao, S.: Agriculture under Climate Change in China: Mitigate the Risks by Grasping the Emerging Opportunities, *Human and Ecological Risk Assessment: An International Journal*, 21, 1259–1276, <https://doi.org/10.1080/10807039.2014.955392>, 2015.
- 595 Toohey, M. and Sigl, M.: Volcanic stratospheric sulfur injections and aerosol optical depth from 500 BCE to 1900 CE, *Earth Syst. Sci. Data*, 9, 809–831, <https://doi.org/10.5194/essd-9-809-2017>, 2017.
- Toohey, M., Krüger, K., Sigl, M., Stordal, F., and Svensen, H.: Climatic and societal impacts of a volcanic double event at the dawn of the Middle Ages, *Climatic Change*, 136, 401–412, <https://doi.org/10.1007/s10584-016-1648-7>, 2016.
- 600 Wang, P. K., Lin, K.-H. E., Lin, Y.-S., Lin, H.-J., Pai, P.-L., Tseng, W.-L., Huang, H.-C., and Lee, C.-R.: Reconstruction of the Temperature Index Series of China in 1368-1911 based on REACHES database, *Scientific data*, 11, 1117, <https://doi.org/10.1038/s41597-024-03937-2>, 2024.
- Wang, P. K., Lin, K.-H. E., Liao, Y.-C., Liao, H.-M., Lin, Y.-S., Hsu, C.-T., Hsu, S.-M., Wan, C.-W., Lee, S.-Y., Fan, I.-C., Tan, P.-H., and Ting, T.-T.: Construction of the REACHES climate database based on historical documents of China, *Scientific data*, 5, 180288, <https://doi.org/10.1038/sdata.2018.288>, 2018.
- 605



- Warren, R.: Climate, crisis, and colonialism: Volcanic eruptions and the causes of famine in British India, 1831 to 1838, *Journal of Historical Geography*, 91, 18–36, <https://doi.org/10.1016/j.jhg.2025.11.005>, 2026.
- Wei, Z. and Li, B.: Relationship between Famine and Climatic Disasters in China during the Qing Dynasty, *Weather, Climate, and Society*, 16, 171–183, <https://doi.org/10.1175/WCAS-D-23-0048.1>, 2024.
- 610 Yang, Z. and Ludlow, F.: Climatic and societal impacts of volcanic eruptions in the Western Han Dynasty (206 BCE–8 CE): a comparative study, *Clim. Past*, 21, 2061–2081, <https://doi.org/10.5194/cp-21-2061-2025>, 2025.
- Yin, F., Sun, Z., You, L., and Müller, D.: Determinants of changes in harvested area and yields of major crops in China, *Food Sec.*, 16, 339–351, <https://doi.org/10.1007/s12571-023-01424-x>, 2024.
- 615 Zhang, D. (Ed.): *A Compendium of Chinese Meteorological Records of the Last 3,000 Years*, 2nd ed., Phoenix House. Ltd., Nanjing, China, 2013.
- Zhu, F., Emile-Geay, J., Anchukaitis, K. J., Hakim, G. J., Wittenberg, A. T., Morales, M. S., Toohey, M., and King, J.: A re-appraisal of the ENSO response to volcanism with paleoclimate data assimilation, *Nature communications*, 13, 747, <https://doi.org/10.1038/s41467-022-28210-1>, 2022.
- 620 Zhuo, Z., Kirchner, I., and Cubasch, U.: Mechanisms of hydrological responses to volcanic eruptions in the Asian monsoon and westerlies-dominated subregions, *Clim. Past*, 19, 835–849, <https://doi.org/10.5194/cp-19-835-2023>, 2023.